Babeş-Bolyai University
Faculty of Chemistry and Chemical Engineering
Doctoral School of Chemistry

Enzymology and Applied Biocatalysis Research Center, RO-400028 Cluj-Napoca, Arany János 11, Romania

Doctoral Thesis Abstract

Engineered PALs for preparative- scale production of L- and D- phenylalanine analogues

PhD candidate: SOUAD-DIANA TORK

Scientific advisor: Prof. Dr. Eng. FLORIN-DAN IRIMIE

Cluj-Napoca, 2023

DOCTORAL THESIS ABSTRACT:

ENGINEERED PALS FOR PREPARATIVE-SCALE PRODUCTION OF L- AND D- PHENYLALANINE ANALOGUES

PhD candidate: **SOUAD-DIANA TORK**

President:

Prof. Dr. Eng. Tiberiu FRENȚIU – Faculty of Chemistry and Chemical Engineering, Babeș-Bolyai University, Cluj-Napoca

Scientific advisor:

Prof. Dr. Eng. Florin-Dan IRIMIE – Faculty of Chemistry and Chemical Engineering, Babeș-Bolyai University, Cluj-Napoca

Reviewers:

Prof. Dr. Bioing. Anca-Irina GALACTION – "Grigore T. Popa" University of Medicine and Pharmacy, Faculty of Medical Bioengineering, Iași

Prof. Dr. Ferencz KILÁR – Institute of Bioanalysis, Faculty of Medicine, University of Pécs, Hungary

Prof. Dr. Eng. Francisc PÉTER – Faculty of Industrial Chemistry and Environmental Engineering, Politechnical University of Timișoara

---

Date: April 28th, 2023
Location: Babeș-Bolyai University, Faculty of Chemistry and Chemical Engineering, Cluj-Napoca

Table of Contents

List of publications

The present thesis is based on the following publications:

1. Tork S.D., Nagy E.Z.A., Cserepes L., Bordea D.M., Nagy B., Toşa M.I., Paizs C., Bencze L.C., The production of L- and D-phenylalanines using engineered phenylalanine ammonia lyases from *Petroselinum crispum*, *Scintific Reports* **2019**, *9*: 20123.
DOI: 10.1038/s41598-019-56554-0
IF: 4.16
ISSN: 2045-2322
AIS: 1.285 (Q1)

2. Tork S.D., Moisă M.E., Cserepes L., Filip A., Nagy L.C., Irimie F.D., Bencze L.C., Towards a general approach for tailoring the hydrophobic binding site of phenylalanine ammonia-lyases, *Scintific Reports* **2022**, *12*: 10606.
DOI: 10.1038/s41598-022-14585-0
IF: 4.54
ISSN: 2045-2322
AIS: 1.285 (Q1)

3. Tork S.D., Nagy E.Z.A., Cserepes L., Tomoiagă R.B., Bencze L.C., Engineered, scalable production of optically pure L-phenylalanines using phenylalanine ammonia-lyase from *Arabidopsis thaliana*, *The Journal of Organic Chemistry* **2023**, *88*: 852
DOI: 10.1021/acs.joc.2c02106
IF: 4.198
ISSN: 0022-3263
AIS: 0.793 (Q1)

Other co-authored publications with complementary topics:

1. Filip A., Nagy E.Z.A., **Tork S.D.**, Bánóczi G., Toşa M.I., Irimie F.D., Poppe L., Csaba P., Bencze L.C., Tailored mutants of phenylalanine ammonia-lyase from *Petroselinum crispum* for the synthesis of bulky L- and D-arylalanines, *ChemCatChem*, **2018**, *10:* 2627.
DOI: 10.1002/cctc.201800258
IF: 4.495
ISSN: 1867-3899
AIS: 1.056 (Q2)

2. Nagy E.Z.A., **Tork S.D.**, Lang P.A., Irimie F.D., Poppe L., Toşa M.I., Schofield C.J., Brem J., Paizs C., Bencze L.C., Mapping the hydrophobic substrate binding site of phenylalanine ammonia-lyase from *Petroselinum crispum*, *ACS Catalysis*, **2019**, *9*: 8825.
DOI: 10.1021/acscatal.9b02108
IF 12.350
ISSN 2155-5435
AIS: 3.13 (Q2)

3. Tomoiagă R.B., **Tork S.D.**, Horváth I., Filip A., Nagy L.C., Bencze L.C., Saturation mutagenesis for phenylalanine ammonia lyases of enhanced catalytic properties, *Biomolecules*, **2020**, *10*: 838.
DOI: 10.3390/biom10060838
IF: 4.555
eISSN: 2218-273X
AIS: 1.041 (Q2)

4. Tomoiagă R.B., **Tork S.D.**, Filip A., Nagy L.C., Bencze L.C., Phenylalanine ammonia lyases: protein engineering versus natural diversity, *Applied Microbiology and Biotechnology*, **2023**, *107:* 1243
DOI: 10.1007/s00253-023-12374-x
IF: 5.46
ISSN: 0175-7598
AIS: 0.864 (Q2)

Thesis objectives

The main **aim of the thesis** is the development of highly efficient biotechnological procedure for the gram-scale synthesis of several unnatural phenylalanine analogues with significant industrial applications using engineered phenylalanine ammonia-lyase (PALs) biocatalysts. A **set of objectives** have been identified and categorized into three distinct chapters, each chapter representing a different aspect of the overall goal:

Objective 1: Development of highly efficient procedure for the synthesis of phenylalanine derivatives using *Pc*PALs, in order to provide empirical evidence for the synthetic utility of the *Pc*PAL mutant variants for practical applications in the synthesis of compounds of high industrial value.

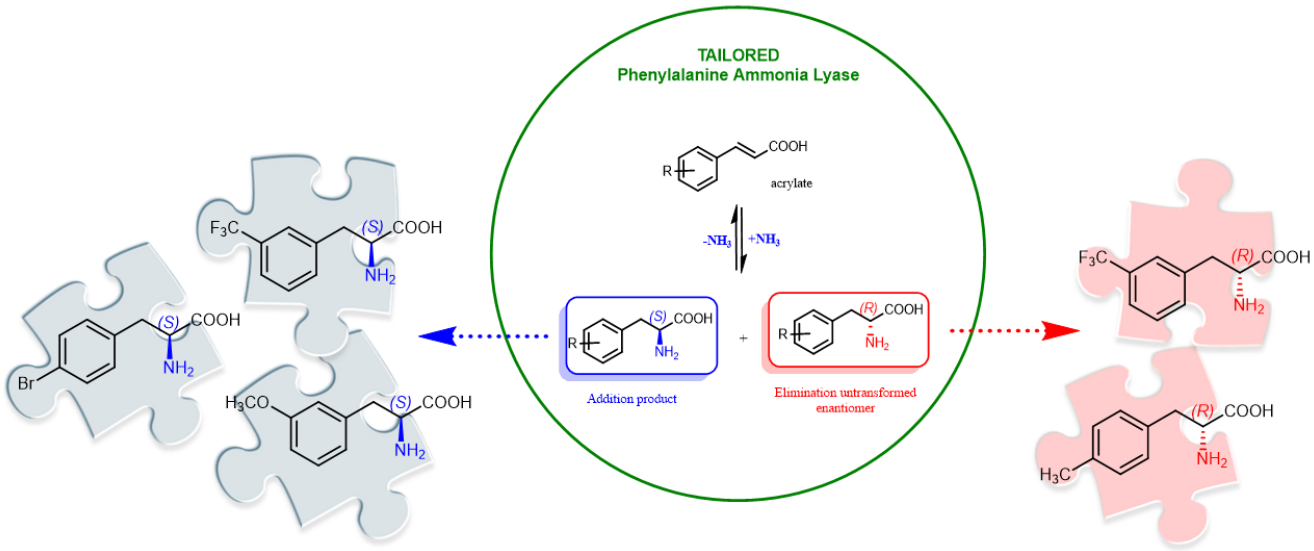

Objective 2: Assessing the transferability of the rational design template that was utilized to produce efficient *Pc*PAL mutant variants as biocatalysts, by examining the extent to which this method can be applied to other PALs within the same enzyme family, in order to provide a range of biocatalysts available for the synthesis of valuable phenylalanine derivatives.

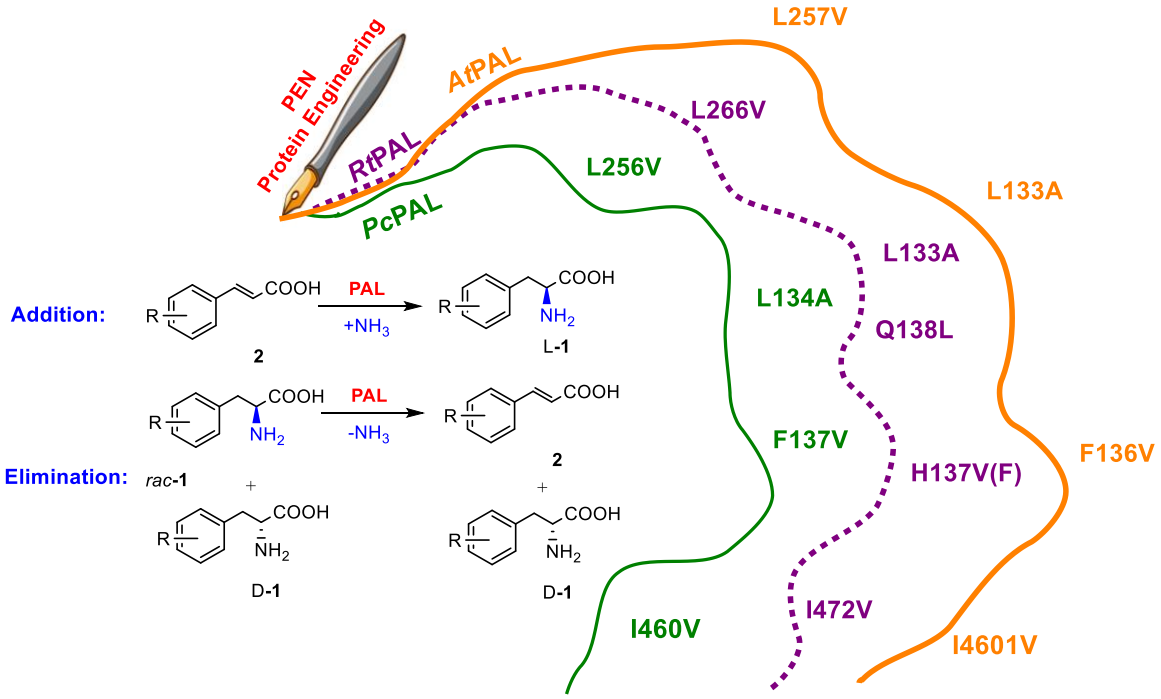

Objective 3: The use of *At*PAL mutant variants to enable the development of a highly efficient engineered biocatalytic procedure that provides cost-effective access to valuable amino acid building blocks and aligns with the principles of sustainable and green chemistry.

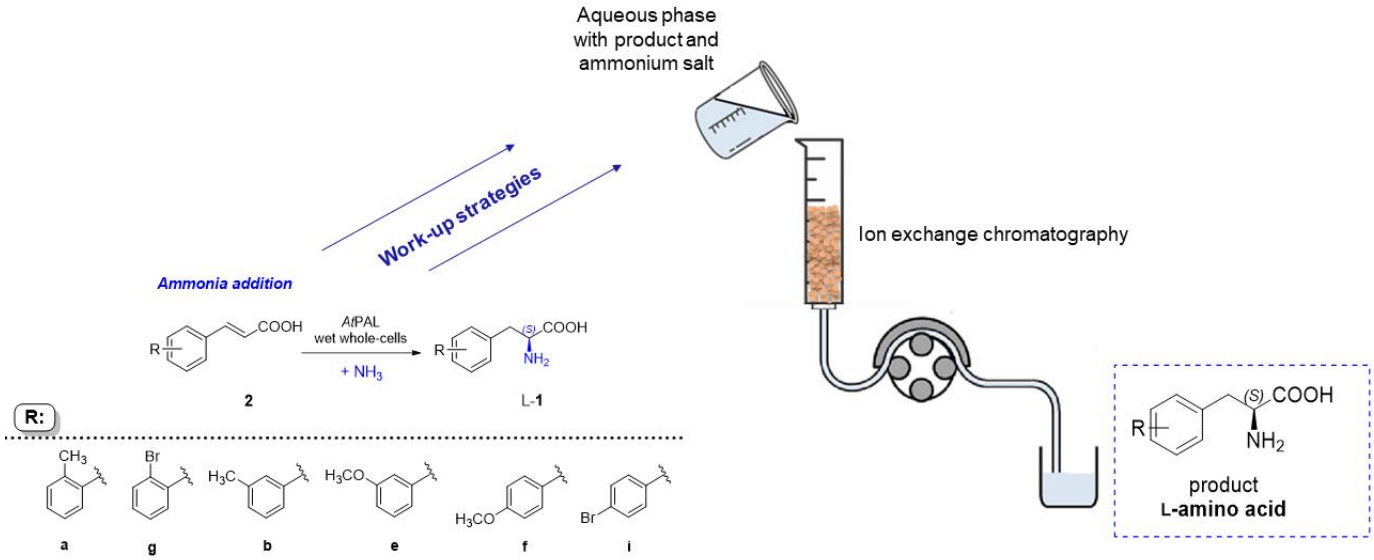

Keywords: unnatural amino acids, phenylalanine ammonia-lyase, preparative-scale, biotransformation, phenylalanine derivatives, protein engineering, sustainable & green synthetic procedures.

CHAPTER I. Introduction: PAL-mediated biotransformations

I.1 Unnatural amino acids as building blocks

Pharmaceutical and fine chemicals companies are actively involved in the production of optically pure amino acids due to their pivotal role as building blocks in the synthesis of various pharmaceuticals, cosmetics, hormones and agrochemicals.[1, 2] The incorporation of non-proteinogenic amino acids into these products has gained significant attention in modern drug discovery research, owing to their structural diversity, but also functional versatility.[2, 3] Peptidomimetics, in particular, have widely employed unnatural amino acids to regulate the natural response or biological activity of targeted products.[2] Additionally, unnatural amino acids have been incorporated into various products, including protease inhibitors for HIV prevention, antibiotics, antimicrobial peptides, antibody-drug conjugates, neuronal receptor ligands and anticancer drugs.[2, 4-6]

Several approaches have been developed for the production of non-proteinogenic amino acids, with chemical synthesis being a widely used method. However, it often results in a racemic mixture of a racemic mixture of D- and L-enantiomers. The separation of these enantiomers is a tedious and challenging task. However, chemical synthesis often yields a racemic mixture of D- and L-enantiomers, which require laborious separation.[2, 7] In contrast, stereoselective chemical and biocatalytic procedures offer an attractive alternative for synthesizing optically pure amino acids, including non-natural amino acids. Biocatalytic methods have gained significant attention in recent years for the synthesis of optically pure amino acids due to their numerous benefits. For instance, biocatalytic methods often use environmentally friendly and mild reaction conditions, allowing the use of readily available and achiral starting materials. Moreover, biocatalysis eliminates the need for protection and/or deprotection steps, which are commonly required in organic synthetic procedures.[1, 2, 7] These advantages have led to the increased interest in the biocatalytic approach for synthesizing optically pure amino acids for various applications in the pharmaceutical and fine chemicals industries.

Of particular interest are aromatic amino acids, such as **phenylalanine derivatives** (the object of this thesis), with several industrial applications such as: food additives[8, 9], cosmetics[10], medicine[11-13] and pharmaceutical applications.

I.2 Phenylalanine ammonia-lyase (PAL)

PAL catalyzes the reversible deamination of L-phenylalanine to *trans*-cinnamic acid, the first step in the biosynthesis of a wide range of phenylpropanoid compounds. The most studied phenylalanine ammonia-lyases are *Rg*PAL (*Rhodotorula glutinis* - yeast PAL)[14], *Rt*PAL (*Rhodosporidium toruloides* - yeast PAL)[15], *Pc*PAL (*Petroselinum crispum* - plant PAL)[16, 17] and *Av*PAL (*Anabaena variabilis* - bacteria PAL)[18].

The substrate scope of *Pc*PAL has been extensively explored, revealing its broad substrate tolerance and potential industrial value in the biocatalytic synthesis of non-natural amino acids. The earlier work of Rétey, Paizs and co-workers has demonstrated the synthesis of several 5-phenylfuran-2-yl-acrylic acids and their corresponding amino acids using purified *wild-type Pc*PAL enzyme, exhibiting excellent conversion and enantiomeric excess (*ee*>99%).[19] *Pc*PAL was also probed with

furan and thiophene systems, including larger fused aromatic rings, converting many of these substrates efficiently with good isolated yields (49-89% in case of ammonia additions and 43-45% in case of ammonia elimination) (**Figure I.1**), despite some previously showing poor or no activity with fungal PALs.[20] However, substrates containing 3-substituted furans and thiophenes were found to adopt an unfavorable binding conformation in the active site, leading to a lack of activity, supporting the Friedel-Crafts-like mechanism.

By thoroughly exploring the active site of *Pc*PAL and demonstrating its broad substrate tolerance, this study has paved the way for the development of potential sustainable routes for the production of a wide range of non-natural amino acid derivatives. Recently, modification of the catalytic site of phenylalanine ammonia-lyase from *Petroselinum crispum* through genetic engineering provided novel mutant variants with enhanced biocatalytic activity. Therefore, engineered F137V mutant has proven to be efficient towards sterically demanding phenylalanine analogues such as styrylalanines[21], while valuable phenylalanine analogues, such as (4-methoxyphenyl)-, (napthalen-2-yl)-, ([1,1'-biphenyl]-4-yl)-, (4'-fluoro-[1,1'-biphenyl]-4-yl)-, and (5-phenylthiophene-2-yl)alanines were synthesized with relatively good yields (19-65%) using combined mutation of F137 and I460 residues[22] (**Figure I.1**). By modifying the hydrophobic binding pocket of *Pc*PAL and assessing a set of single mutant variants, improved activity and selectivity were achieved towards phenylalanines and cinnamic acids substituted with electron-donating or electron-withdrawing groups at all positions (*ortho*, *meta*, *para*) on their aromatic ring.[23]

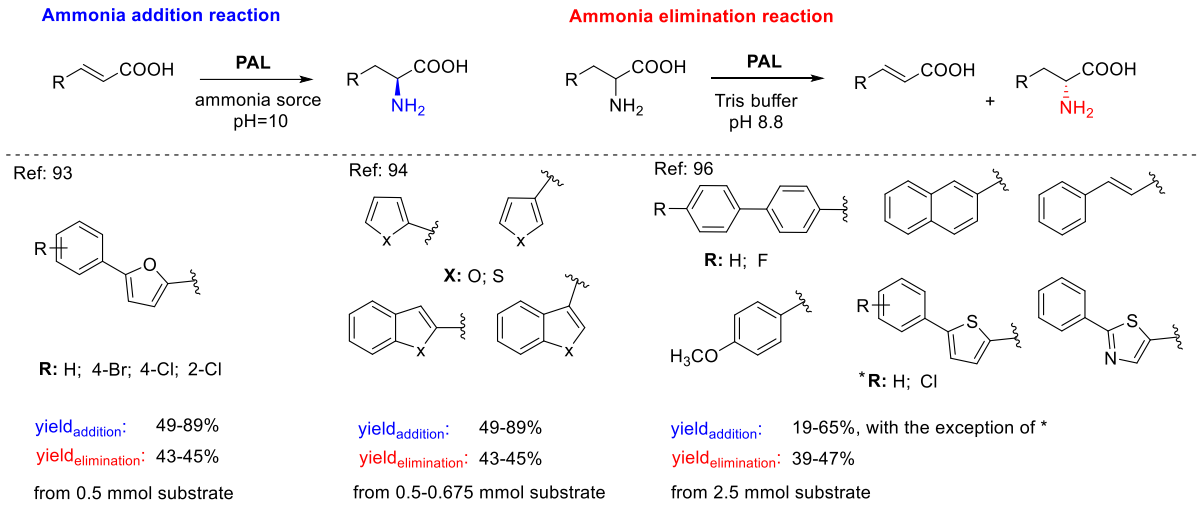

Figure I.1. Reported preparative-scale ammonia addition and elimination reactions using *Pc*PAL enzyme.

I.3 The current state-of-the-art of scalable PAL-mediated biotransformations

One of the significant advantages of using phenylalanine ammonia-lyases (PALs, EC 4.3.1.24/25) in chemical synthesis is their ability to catalyze the addition of ammonia to *trans*-cinnamic acids, even at high ammonia concentrations. This unique property enables the asymmetric synthesis of optically pure L-phenylalanine analogues, making PALs an attractive biocatalyst for the production of chiral amino acids.

Although, PAL-catalyzed reactions have shown promise in chemical synthesis, there is a limited number of examples of successful and scalable amination reactions using these biocatalysts. Royal DSM, a life science and materials company, has developed a successful industrial-scale

amination reaction for the production of the key intermediate (*S*)-2,3-dihydro-1*H*-indole-2-carboxylic acid used in the synthesis of ACE inhibitors, which are commonly used to treat hypertension.[24] The reaction involves selective amination of 2-Cl- or 2-Br-cinnamic acids using a PAL enzyme from *Rhodotorula glutinis* (*Rg*PAL) and copper-catalyzed ring closure to give (*S*)-2-indolinecarboxylic acid. The reaction produces 18.1 g (100 mM) of 2-Cl-(*S*)-α-phenylalanine with 91% conversion in 8.5 hours (**Figure I.2**).

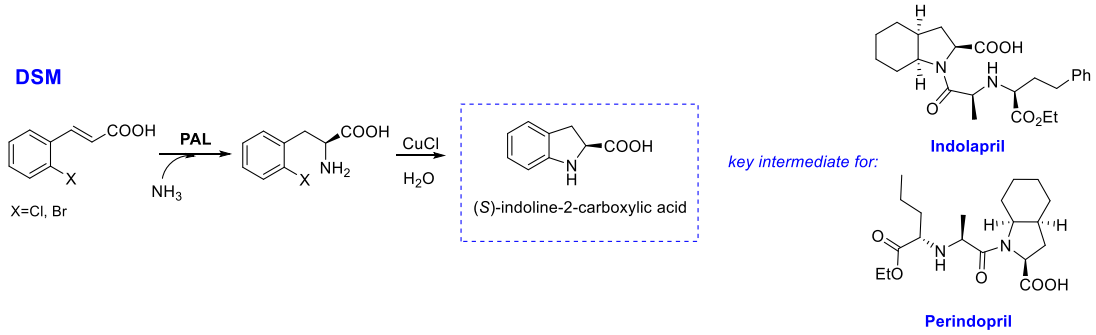

Figure I.2. Multi-ton scale production of (*S*)-2,3-dihydro-1*H*-indole-2-carboxylic acid by DSM.

Another engineered *Av*PAL enzyme (PAL-130 SEQ ID NOs 987/988, developed by Codexis, using their CodeEvolver protein engineering platform) was used in the optimized synthesis of Olodanrigan (EMA401), an angiotensin II type 2 antagonist used to treat postherpetic neuralgia and neuropathic pain. Novartis developed a synthetic approach for EMA401 that involves the hydroamination of (*E*)-3-(2-(benzyloxy)-3-methoxyphenyl)acrylic acid to (*S*)-2-amino-3-(2-(benzyloxy)-3-methoxyphenyl)propanoic acid as the key step. The PAL-130 enzyme was applied under optimal conditions for the biotransformation of a cinnamic acid derivative, resulting in the production of the tetrahydroisoquinoline intermediate in a 68% yield after four days[25] (**Figure I.3**).

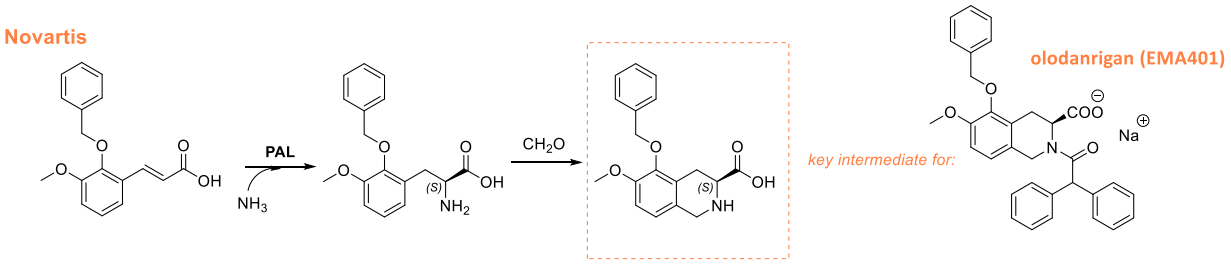

Figure I.3. Biocatalytic route to EMA401 by Novartis.[25]

CHAPTER II. The production of L- and D-phenylalanines using engineered phenylalanine ammonia-lyases from *Petroselinum crispum*

II.1 Background (literature data)

II.2 Results and Discussion

The production of several important (*S*)-α-phenylalanine and (*R*)-α-phenylalanine analogues using the reported mutant variants of *Pc*PAL (L256V, L134A and I460V)[23] (**Figure II.1**) required us to establish the optimal conditions for the preparative-scale biotransformations. Accordingly, several reaction parameters were optimized for both ammonia addition and elimination reactions: biocatalysts: substrate ratio, reaction medium/ammonia source and substrate concentration.

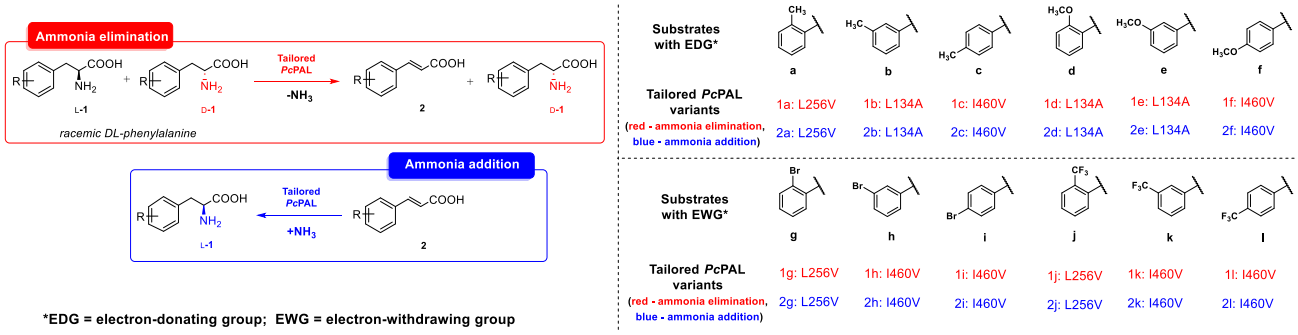

Figure II.1. Tested substrates in the ammonia addition and ammonia elimination reactions of mono-substituted cinnamic acids and racemic phenylalanines with electron-donating (-CH_3, -OCH_3) or electron-withdrawing (-CF_3, -Br) substituents, catalyzed by the corresponding *Pc*PAL mutant variants[23].

II.2.1 Optimization of *Pc*PAL-based amination reactions

II.2.1.1 The effect of reaction medium/ammonia source

The influence of the reaction medium utilized as ammonia source as well as reaction buffer on the conversion and enantiomeric excess values of hydroamination reactions was studied using two *para*-substituted cinnamic acid derivatives, *p*-methyl-cinnamic acid **2c** and *p*-trifluoromethyl-cinnamic acid **2l** as model substrates. The ammonia additions were performed at a fixed substrate concentration of 2 mM and whole-cell *Pc*PAL I460V-biocatalysts in cell densities of OD_{600} ~ 1 (~6 mg wet cells/mL), varying different concentration of ammonia buffer solutions (2, 4, 6 M NH_4OH pH 10.0 adjusted with CO_2) and ammonium carbamate buffer solutions (2, 4, 6 M $NH_4[H_2NCO_2]$ pH ~10.0 without adjustment).

The results obtained from the ammonia addition reactions of substrates **2c** and **2l** indicate that the highest conversions were achieved using 6 M NH_4OH, with conversion values of 30.2% and 60.3%, respectively after 24 h reaction time (**Figure II.2**). However, the use of 4-6 M $NH_4[H_2NCO_2]$ resulted in significantly lower conversion values (11.1-20.6% for **2c** and <1-17.6% for **2l**, respectively) after 24 hours, contrarily to previously reported PAL-based amination reactions[26, 27]. The results shown in **Figure II.2** indicate that the use of 2 M ammonium carbamate solution resulted in comparable conversion values to those achieved in a 6 M ammonia buffer. This outcome is most likely due to the fact that $NH_4[H_2NCO_2]$ releases twice as many ammonia molecules and has a lower overall ionic strength compared to NH_4OH.

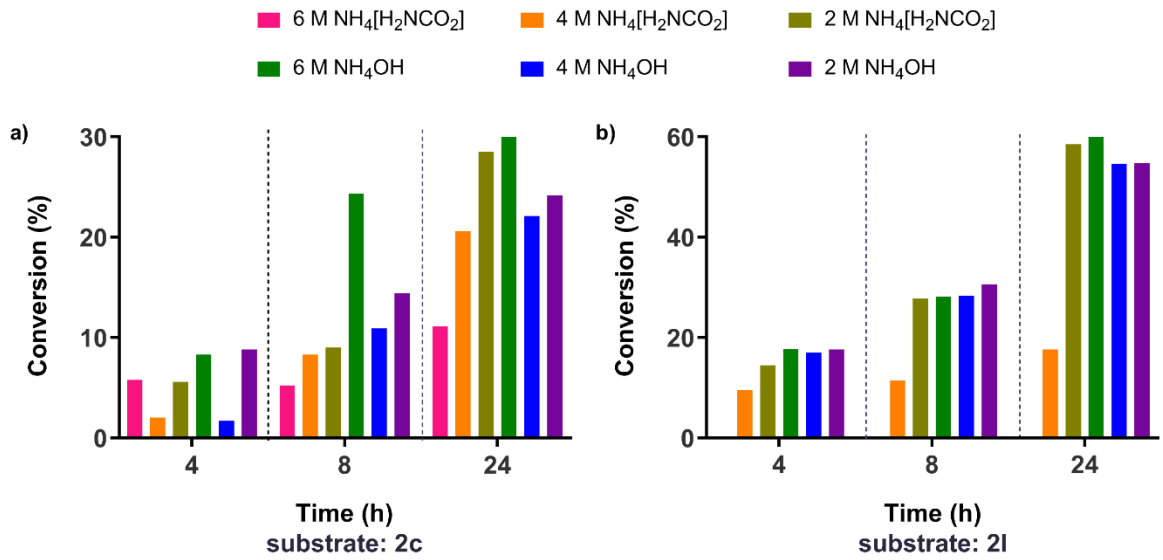

Figure II.2. Conversion values obtained in the ammonia addition reactions of a) *p*-CH_3-cinnamic acid **2c** and b) *p*-CF_3-cinnamic acid **2l**, using NH_4OH and $NH_4[H_2NCO_2]$ as ammonia sources. In all points of the reactions the enantiomeric excess (*ee*) values were >99%.

II.2.1.2 The effect of cell density/biocatalyst: substrate ratio

The effect of different cell densities upon conversion and enantiomeric excess (*ee*) values was tested for the same model substrates: *p*-methyl-cinnamic acid **2c** and *p*-trifluoromethyl-cinnamic acid **2l**. Whole-cell *Pc*PAL I460V-biocatalysts in cell densities of OD_{600} ~ 1, 2, 4, and 8 correspond to a wet cell concentration of ~ 6, 12, 24 and 48 mg/mL, respectively. At a fixed substrate concentration of 2 mM, the biocatalyst: substrate ratio (OD_{600}: mM) varied from 0.5 to 4. Using a cell density of OD_{600} ~2 resulted in high conversion values (**Figure II.3**), while increasing the cell density to OD_{600} ~4 or 8 only led to an increase of reaction medium viscosity, making sample preparation, reaction work-up and HPLC monitoring difficult. Hence, a biocatalyst: substrate ratio (OD_{600}: mM) of 1 was chosen for further optimization.

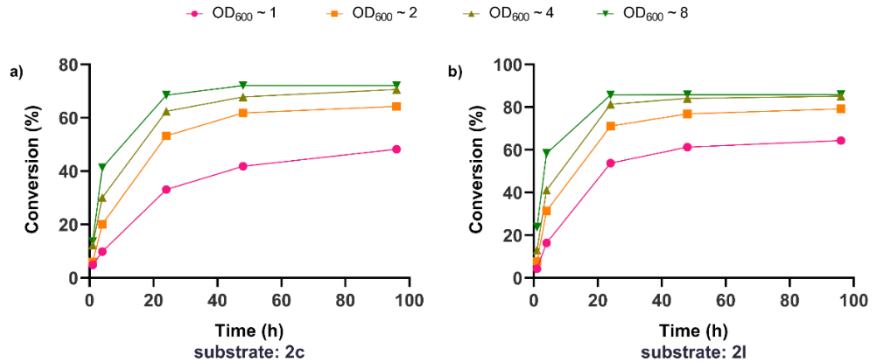

Figure II.3. Conversion values obtained in the ammonia addition reactions of a) *p*-CH_3-cinnamic acid **2c** and b) *p*-CF_3-cinnamic acid **2l** by varying the biocatalyst: substrate ratio (OD_{600}: mM).

II.2.1.3 The effect of substrate concentration

The effect of substrate concentration on the catalytic performance of the engineered *Pc*PAL mutant variants (L134A, L256V and I460V) was tested in the ammonia addition onto all cinnamic acid analogues **2a-l** in the limit of their solubilities for 48 hours, using 6 M NH_4OH as reaction medium and ammonia source and an optimal biocatalyst: substrate ratio (OD_{600}: mM) of ~1.

The results show that *ortho*-substituted substrates (except *o*-CH_3-cinnamic acid) exhibited high conversions even at high substrate concentrations up to 70 mM after 48 hours of reaction time, with conversion values of 91.8% for **2a**, 81.0% for **2g**, and 66.0% for **2j** (**Figure II.4**). However, the conversion values for *o*-OCH_3-cinnamic acid **2d** dropped from 44.4% to 19.9% upon doubling the substrate concentration from 10 mM to 20 mM (**Figure II.4**).

In case of *meta*-substituted substrates bearing electron-withdrawing -CF_3 and -Br groups, the maximal stationary conversion approached ~80% after 24 h at low substrate concentration of 2 and 5 mM, respectively (**Figure II.5**). The ammonia addition reaction of *m*-CH_3-cinnamic acid **2b** stopped at 26.4% at a low substrate concentration of 2 mM after 48 h. However, the stationary conversion value for *m*-OCH_3-cinnamic acid **2e** was not affected by the increase in substrate concentration and reached 71% at 50 mM after 48 h (**Figure II.5**).

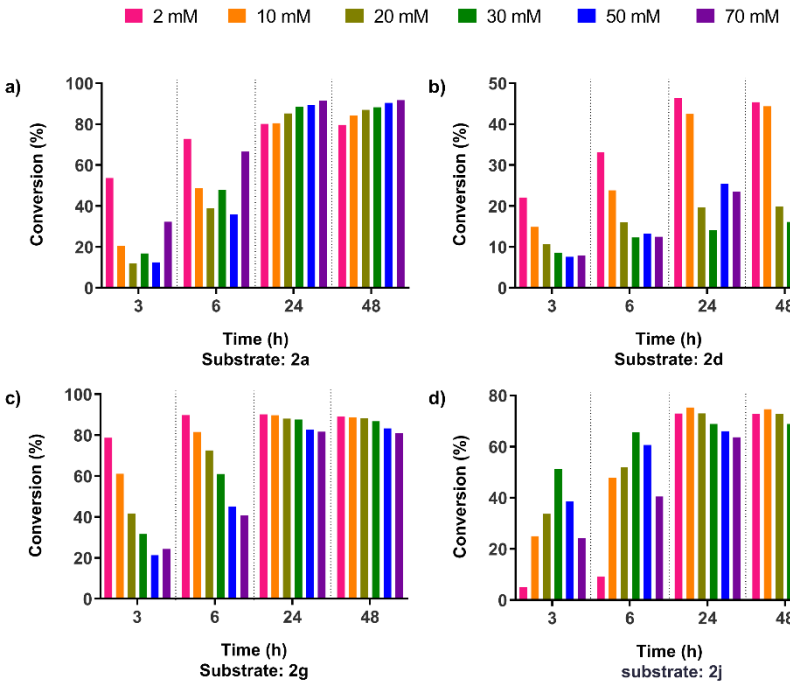

Figure II.4. Time conversion profiles for the ammonia addition reactions onto a) *o*-CH_3-cinnamic acid **2a**, b) *o*-OCH_3-cinnamic acid **2d**, c) *o*-Br-cinnamic acid **2g** and d) *o*-CF_3-cinnamic acid **2j** using the corresponding mutant *Pc*PAL variants.

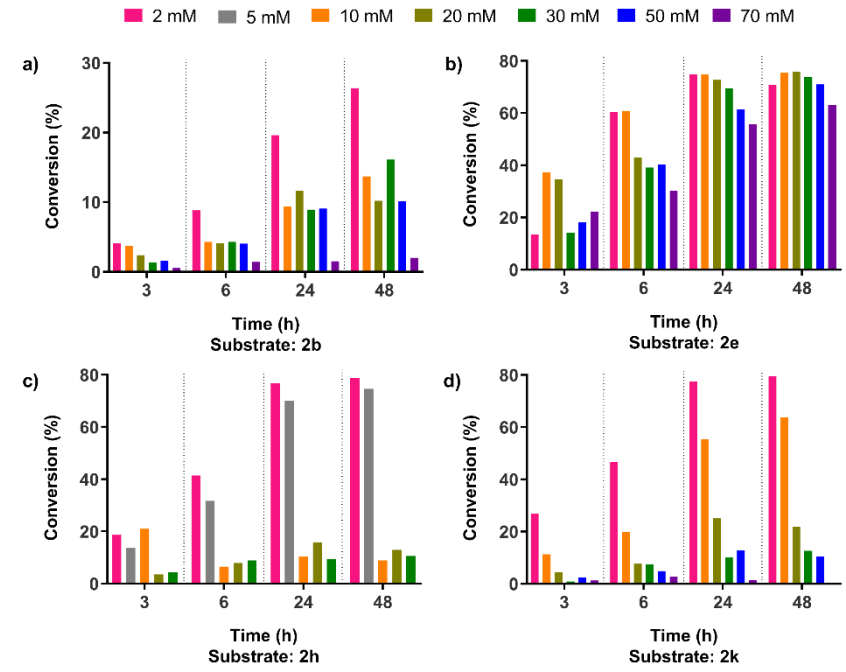

Figure II.5. Time conversion profiles for the ammonia addition reactions onto a) *m*-CH_3-cinnamic acid **2b**, b) *m*-OCH_3-cinnamic acid **2e**, c) *m*-Br-cinnamic acid **2h** and *m*-CF_3-cinnamic acid **2k** using the corresponding mutant *Pc*PAL variants.

Similar situation was observed for *p*-OCH_3-cinnamic acid **2f**, where the amination reaction stopped at a low stationary conversion of only 19.1% at 30 mM substrate concentration after 48 h (**Figure II.6**). Exception, moderate conversion values (~55-60%) were maintained at substrate concentration as high as 50 mM in case of *p*-CH_3-cinnamic acid **2c**.

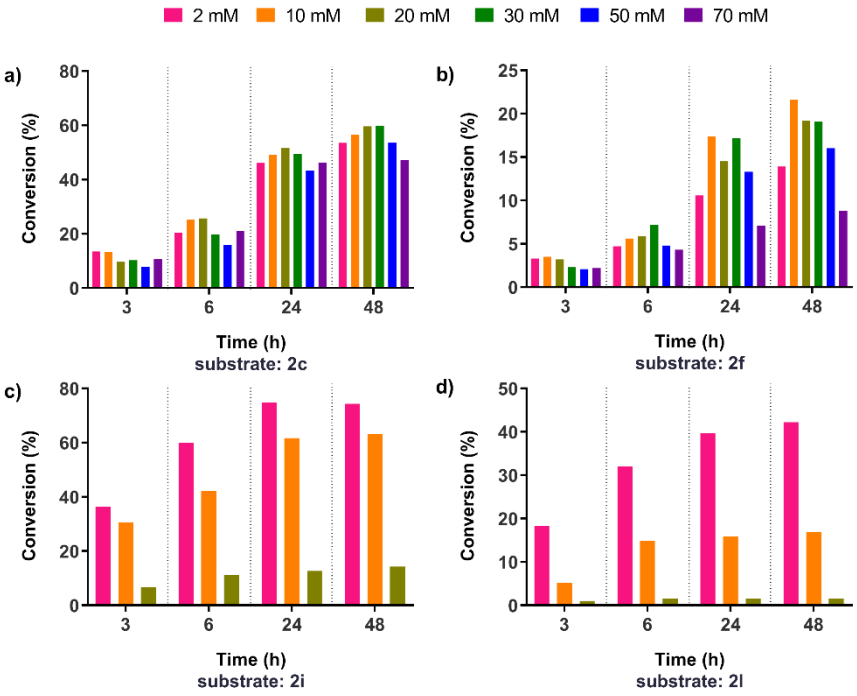

Figure II.6. Time conversion profiles for the ammonia addition reactions onto a) *p*-CH_3-cinnamic acid **2c**, b) *p*-OCH_3-cinnamic acid **2f**, c) *p*-Br-cinnamic acid **2i** and d) *p*-CF_3-cinnamic acid **2l** using the corresponding mutant *Pc*PAL variants.

II.2.1.4 Product/Substrate inhibition

Using the optimized parameters determined for the ammonia addition reactions onto cinnamic acid derivatives **2a-l** high or moderate conversions with excellent enantioselectivities were registered, with two exceptions, such as in case of amination reactions of **2b** and **2f**, where significantly low stationary conversions of 26.4% and 19.1%. The product inhibitory effect was demonstrated by monitoring the production of phenylalanine derivatives in the presence of different concentrations of *rac*-**1b** and *rac*-**1f** (0-1.5 mM), using the optimal conditions and a fixed substrate concentration of **2b** and **2f** of 1 mM (**Figure II.7**). Additionally, the product inhibitory effect in the amination reactions of *p*-CH_3O-cinnamic acid **2f** was also investigated using kinetic measurements, monitoring the formation of phenylalanine derivative L-**1f** at 316 nm by varying different concentrations of *rac*-**1f** (0-2 mM) (**Figure II.8**).

The occurrence of substrate inhibition was also investigated for **2l**, which exhibited reduced stationary conversions at higher substrate concentrations. The inhibition was confirmed by UV-monitoring the production of L-**1l** at 316 nm in the presence of different concentrations of **2l** using purified I460V *Pc*PAL enzyme (**Figure II.8**).

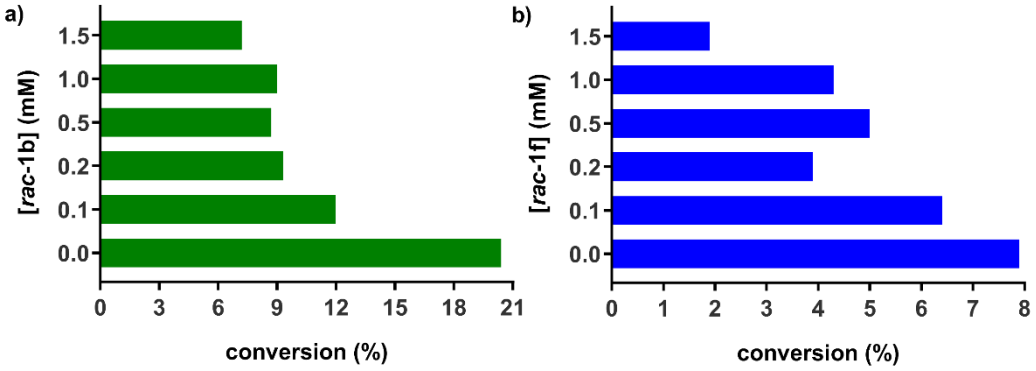

Figure II.7. The influence of increasing product concentration on the conversion values of ammonia addition onto a) *m*-CH_3-cinnamic acid **2b** and b) *p*-CH_3O-cinnamic acid **2f**, respectively using whole-cells of L134A and I460V *Pc*PAL as biocatalyst.

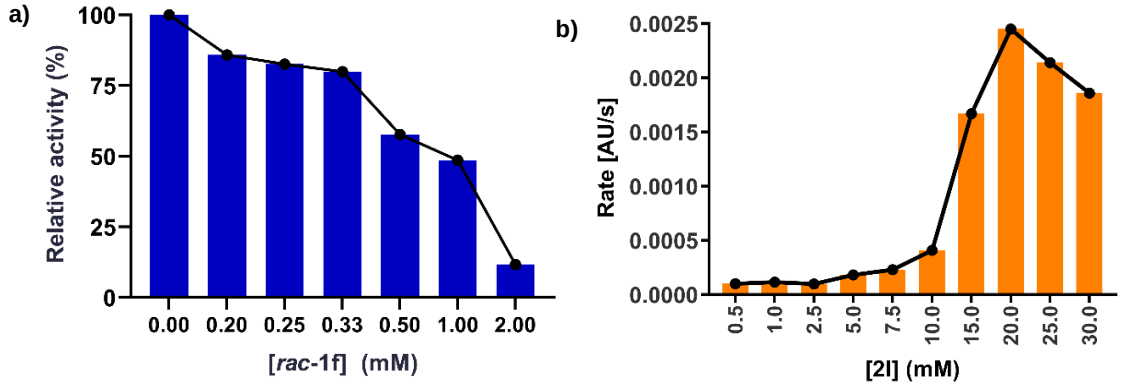

Figure II.8. The influence of increasing a) product concentration on the relative activity of ammonia addition onto **2f** and b) substrate concentration on the reaction velocity of ammonia addition onto **2l**, using purified I460V *Pc*PAL enzyme.

II.2.2 Optimization of *Pc*PAL-based deamination reactions

II.2.2.1 The effect of different buffer systems used as reaction medium

The influence of various buffer systems on the conversion and enantiomeric excess values (ee_D) were studied in the ammonia elimination reactions of model substrates *rac*-*p*-CH_3-phenylalanine (*rac*-**1c**) and *rac*-*m*-CF_3-phenylalanine (*rac*-**1k)** of fixed substrate concentration of 2 mM. The tested aqueous buffer systems, such as Tris (20 mM Tris.HCl, 120 mM NaCl, pH 8.8), NH_4OH (0.1 M NH_4OH, pH 9.5, adjusted with CO_2), phosphate-buffer (0.1 M Na_2HPO_4-NaH_2PO_4, pH 8.8), borax (0.1 M $Na_2[B_4O_5(OH)_4]$, pH 9.5), ammonium acetate (0.1 M CH_3COONH_4, pH 9.5,) and sodium carbonate (0.1 M Na_2CO_3/$NaHCO_3$, pH 9.0) position within the optimal pH domain of PALs that generally vary between 8.2-9.5.[18, 28, 29] The pH profile of I460V *Pc*PAL-whole cells mediated biotransformation was determined in the deamination of *rac*-**1k**, using Tris-buffer as reaction medium with different pH values (pH 7.5–10.0). The highest conversion values (~50%) were obtained after 20 h when using Tris-buffer systems of pH ranging between 8.8-9.7 (**Figure II.9**).

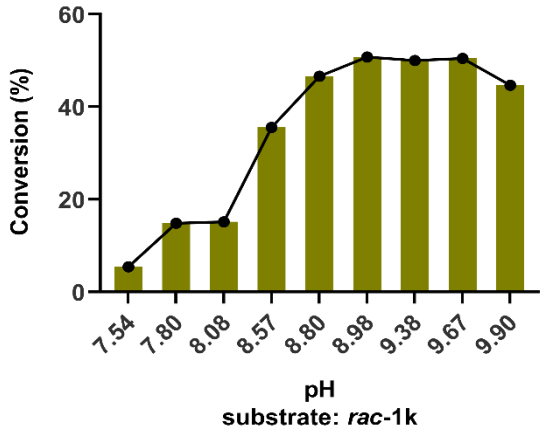

Figure II.9. Conversion values obtained in the *Pc*PAL I460V whole-cells mediated deamination reaction of *rac*-*m*-CF_3-phenylalanine *rac*-**1k** using Tris-buffer as reaction medium (pH value ranges from 7.5 to 10.0).

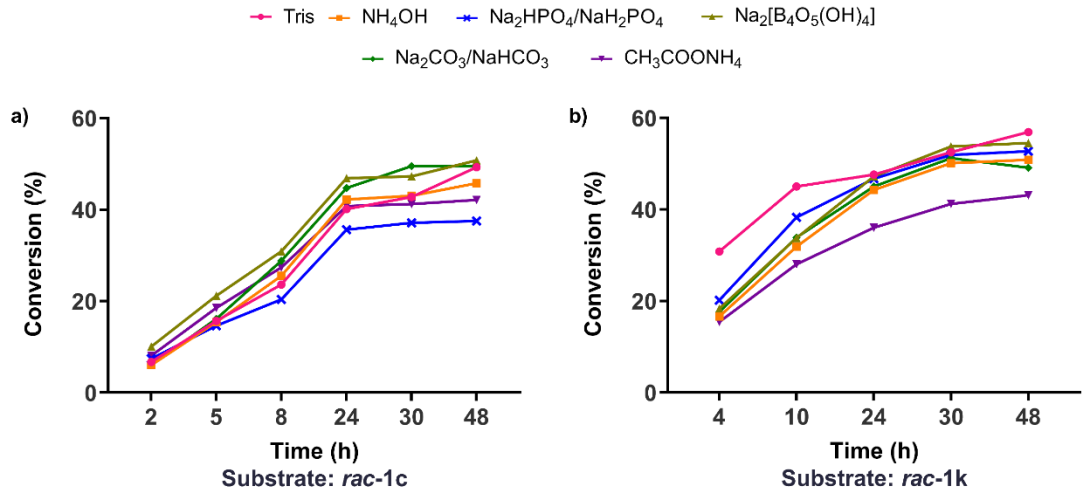

Figure II.10. Conversion values obtained in the *Pc*PAL I460V whole-cells mediated deamination reaction of a) *rac*-*p*-CH_3-phenylalanine *rac*-**1c** and b) *rac*-*m*-CF_3-phenylalanine *rac*-**1k** using different buffer systems as reaction medium.

The optimal buffer system for further optimization reactions was determined to be borax buffer which provided the highest conversion and enantiomeric excess for both model substrates (**Figure II.10**).

II.2.2.2 The effect of reaction medium cell density/biocatalyst: substrate ratio

Table II.1. The effect of increased whole-cell biocatalysts densities upon conversion values and enantiomeric excess of *rac*-*p*-methyl-phenylalanine *rac*-**1c** and *rac*-*m*-trifluoromethyl-phenylalanine *rac*-**1k**.

Substrate	(OD_{600}: mM) ratio of 0.5			(OD_{600}: mM) ratio of 1			(OD_{600}: mM) ratio of 2		
	c (%)	$ee_{D\text{-}1}$ (%)	$ee_{theorD\text{-}1}$ (%)	c (%)	$ee_{D\text{-}1}$ (%)	$ee_{theorD\text{-}1}$ (%)	c (%)	$ee_{D\text{-}1}$ (%)	$ee_{theorD\text{-}1}$ (%)
p-methyl-phenylalanine (*rac*-**1c**)	38.1[#]	63.3	61.7	39.9[#]	66.3	66.5	~50[#]	94.1	>99
m-trifluoromethyl-phenylalanine (*rac*-**1k**)	27.3*	37.5	37.5	45.6*	88.8	84	~50*	>99	>99

Reaction conditions: assays were performed in 1.5 mL polypropylene tubes at 30 °C, 250 rpm, in 500 µL reaction volume, using 2 mM substrate concentration, varied (OD_{600}: mM) ratio and 0.1 M $Na_2[B_4O_5(OH)_4]$, pH 9.5 as buffer solution. [#]after 24 h; *after 5 h;

The effect of biocatalyst: substrate ratio (OD_{600}: mM) was tested on the same model substrates. By maintaining a fixed substrate concentration of 2 mM prepared in borax buffer (0.1 M $Na_2[B_4O_5(OH)_4]$, pH 9.5) the cell density (OD_{600}) was varied from 1 to 4. The increase of biocatalyst: substrate ratio (OD_{600}: mM ratio of 2) led to shorter reaction times for achieving the optimal conversion of 50% (**Table II.1**).

II.2.2.3 The effect of substrate concentration

The influence of substrate concentration on the conversion and *ee* values of model substrates *rac*-**1c** and *rac*-**1k** was tested in the limit of their solubilities. The deamination reactions were performed in 0.1 M $Na_2[B_4O_5(OH)_4]$, pH 9.5 buffer solution with an OD_{600}: mM ratio of 0.5 (in order to reduce reaction medium viscosity), varying the substrate concentration of *rac*-**1c** and *rac*-**1k**.

Optimal conversion of 50% was achieved for *rac*-**1c** regardless of substrate concentration (**Figure II.11**), but a decrease in enantiomeric excess values was observed with increasing substrate concentration (89% at 15 mM substrate concentration) (**Figure II.12**). For *rac*-**1k**, low or no conversions were obtained at high substrate concentrations (>10 mM) (**Figure II.13**) with a significant decrease in enantiomeric excess values.

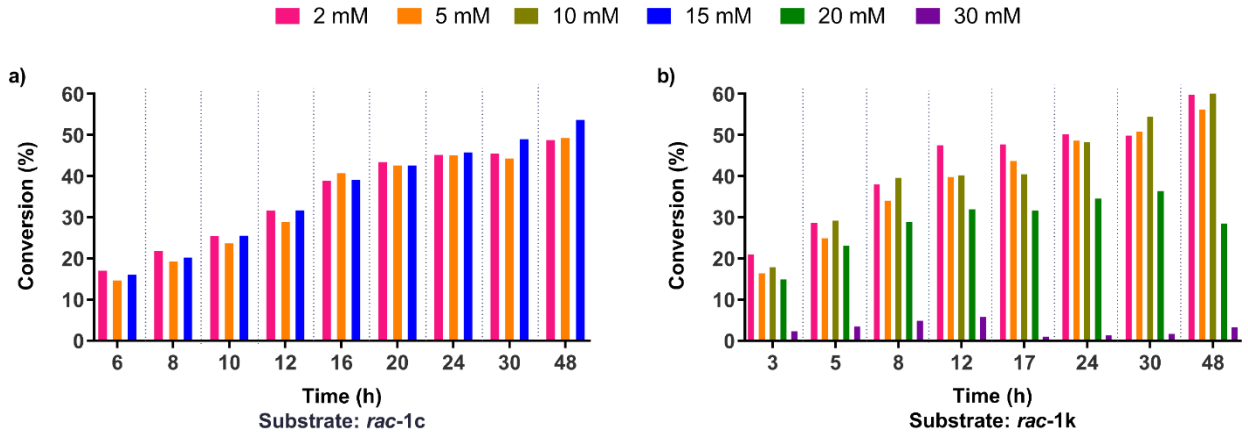

Figure II.11. The influence of increasing substrate concentration on the conversion values of ammonia elimination from a) *rac*-*p*-methyl-phenylalanine *rac*-**1c** and b) *rac*-*m*-trifluoromethyl-phenylalanine *rac*-**1k**, respectively using whole-cells I460V *Pc*PAL as biocatalyst.

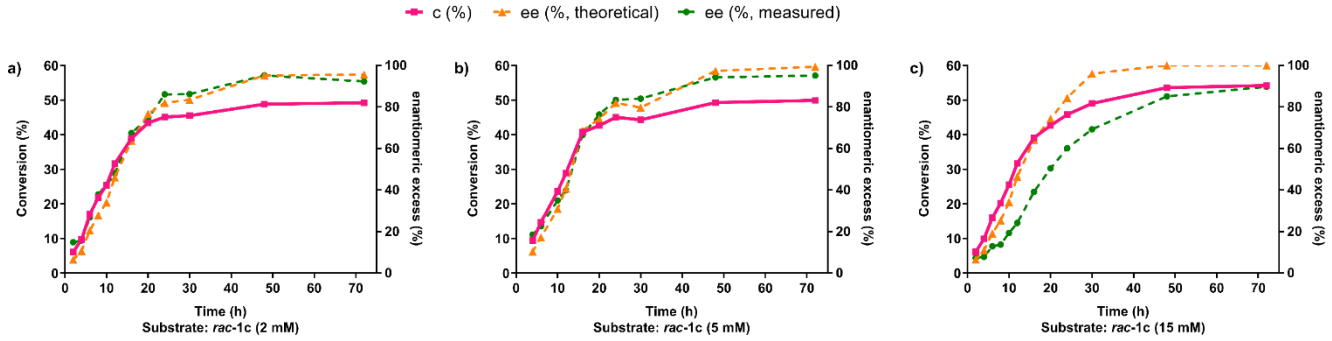

Figure II.12. Time progression profile (conversion- and enantiomeric excess) for the ammonia eliminations from *p*-CH_3-phenylalanine *rac*-**1c** using I460V *Pc*PAL whole-cells as biocatalyst and a) 2 mM, b) 5 mM and c) 15 mM substrate concentration.

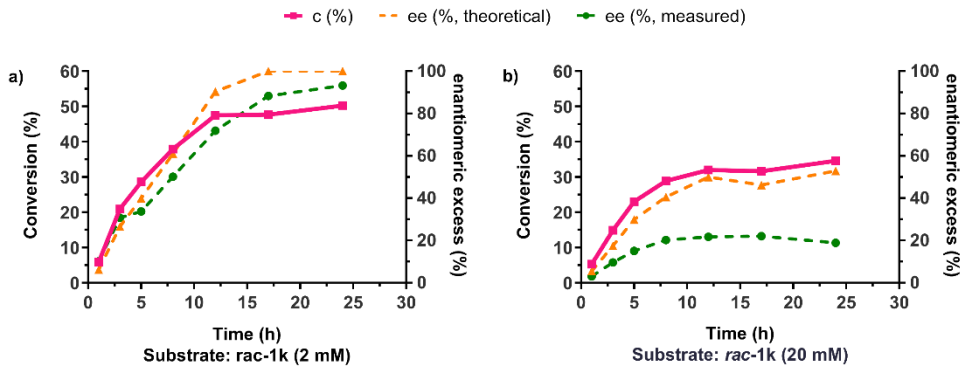

Figure II.13. Time progression profile (conversion and enantiomeric excess) for the ammonia eliminations from *rac*-*m*-CF_3-phenylalanine *rac*-**1k** using I460V *Pc*PAL whole-cells as biocatalyst and a) 2 mM and b) 20 mM substrate concentration.

II.2.2.4 Substrate inhibition

The decrease of conversion values with the increase of substrate concentration suggested the occurrence of substrate inhibition, similarly to the ammonia addition onto *m*-CF_3-cinnamic acid **2k**. Substrate inhibition in the ammonia elimination reaction from *rac*-**1k** was confirmed spectrophotometrically by UV-monitoring the production of *m*-CF_3-cinnamic acid **2k** at 290 nm in the presence on different concentration of *rac*-**1k** (0.1-50 mM), using purified I460V *Pc*PAL enzyme as biocatalyst. In this case, significant decrease of reaction velocities values was registered at substrate concentration higher than 10 mM (**Figure II.14**).

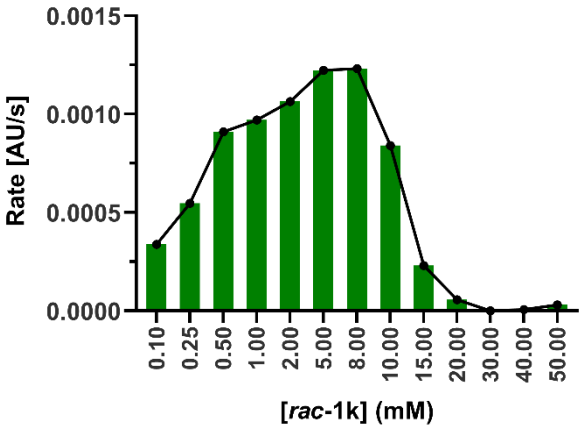

Figure II.14. The influence of increasing substrate concentration on the reaction velocity of ammonia elimination from *rac*-*m*-CF_3-phenylalanine *rac*-**1k** using purified I460V *Pc*PAL enzyme.

II.2.3 Preparative scale ammonia addition and elimination reactions

II.2.3.1 Optimal conditions

In case of amination reactions, the optimal conditions determined were a biocatalyst: substrate ratio (OD_{600}: mM) of 1, 6 M NH_4OH pH 10 (adjusted with CO_2) as reaction medium, while the increase of substrate concentration had an effect on conversion values on most substrates, due to the occurrence of substrate or product inhibition. Therefore, the optimal substrate concentrations were chosen taking into account the highest conversion and enantiomeric excess (*ee*) values obtained in the shortest reaction time (**Table II.2**). In case of cinnamic acid analogues bearing the electron-donor substituent -OCH_3, superior conversions and ee_L values were obtained compared to those reported

for *wild-type Pc*PAL[23] (c<1% for **2d**, **2f** and c=1% for **2e**), *Av*PAL[30] (c=25% for **2e** and c=2% for **2e**) and *Pb*PAL F133A variant[31, 32] (c=30% for **2d**). In case of methyl-substituted cinnamic acids, lower enantiomeric excess and conversion values are reported for *Av*PAL[30] ($ee_{L\text{-}\mathbf{1d}}$=90%, c=64% for **2d**, $ee_{L\text{-}\mathbf{1e}}$=94%, c=58% for **2e** and c=59% for **2f**). In case of cinnamic acids with electron-withdrawing groups, ee_L values exceeded the results obtained previously with *wt-Av*PAL[33] for **2l** ($ee_{L\text{-}\mathbf{1l}}$=76% and c=65%), while conversion values are superior to those reported for *wild-type Av*PAL[30] (c=66% for **2g**, c=55% for **2h** and c=42% for **2i**) and comparable to those obtained with *Av*PAL F107L, F107I and F107A mutants[34] (c=72-80% for **2i**), but surpassed by *Rg*PAL 31E mutant[26] (c=94% for **2i**).

In case of deamination reactions, the optimal conditions determined were a biocatalyst: substrate ratio (OD_{600}: mM) of 0.5, 0.1 M $Na_2[B_4O_5(OH)_4]$, pH 9.5 as reaction medium, while the increase of substrate concentration significantly decreased the conversion values just like in the case of ammonia additions but also had an impact on enantiomeric excess values. Therefore, deamination from *rac*-**1c** and *rac*-**1k** were performed at relatively low substrate concentrations (5 mM and 2 mM, respectively) in order to obtain the optimal 50% conversion value at relatively high ee_D values (95% and 93%, respectively) (**Table II.2**). Substrates marked with grey background were further selected for preparative-scale biotransformations.

Table II.2. Conversion and enantiomeric excess (*ee*) values obtained in the ammonia addition and elimination reactions under optimal conditions.

Reaction	Substrate	Substituent	*Pc*PAL variant	[S] (mM)	Time (h)	c (%)	*ee* (%)*
Ammonia addition	**2a**	*o*-CH_3	L256V	70	24	91.5	>99
	2b	*m*-CH_3	L134A	2	48	26.4	>99
	2c	*p*-CH_3	I460V	30	48	59.9	>99
	2d	*o*-OCH_3	L134A	10	24	42.5	>99
	2e	*m*-OCH_3	L134A	50	48	71.0	>99
	2f	*p*-OCH_3	I460V	30	48	19.1	>99
	2g	*o*-Br	L256V	70	24	81.6	>99
	2h	*m*-Br	I460V	5	24	70.1	98.3
	2i	*p*-Br	I460V	10	24	61.6	>99
	2j	*o*-CF_3	L256V	20	24	73.0	>99
	2k	*m*-CF_3	I460V	2	24	77.5	>99
	2l	*p*-CF_3	I460V	2	48	42.2	>99
Ammonia elimination	***rac*-1c**	*p*-CH_3	I460V	5	48	~50	95
	***rac*-1k**	*m*-CF_3	I460V	2	23	~50	93

Reaction conditions for amination of 2a-l: assays were performed in 1.5 mL polypropylene tubes at 30 °C, 250 rpm, in 500 µL reaction volume, using 2-70 mM substrate concentration, (OD_{600}: mM) ratio of 1.0 and 6 M NH_4OH pH 10 (adjusted with CO_2) as reaction medium.

Reaction conditions for deamination of rac-1c and rac-1c: assays were performed in 1.5 mL polypropylene tubes at 30 °C, 250 rpm, in 500 µL reaction volume, using 2-70 mM substrate concentration, (OD_{600}: mM) ratio of 0.5 and 0.1 M $Na_2[B_4O_5(OH)_4]$, pH 9.5 as buffer solution

*ee_L (addition reaction) and ee_D (elimination reaction)

II.2.3.2 Use of PAL for preparative-scale biotransformations

Using the optimal reaction conditions, preparative-scale biotransformations (500 mg) were performed to confirm the synthetic applicability of the engineered *Pc*PALs.

Model substrates (**2e, 2i** and **2k** for ammonia addition reactions and *rac*-**1c**, *rac*-**1k** for ammonia elimination reactions**)** were selected for the production of enantiopure L- and D-Phe

analogues of high industrial interest such as: (*S*)-2-amino-3-(3-methoxyphenyl)propanoic acid (*S*)-**1e**, (*S*)-2-amino-3-(4-bromophenyl)propanoic acid (*S*)-**1i**, (*S*)-2-amino-3-(3-(trifluoromethyl)phenyl)propanoic acid (*S*)-**1k**, (*R*)-2-amino-3-(*p*-tolyl)propanoic acid (*R*)-**1c** and (*R*)-2-amino-3-(3-(trifluoromethyl)phenyl)propanoic acid (*R*)-**1k**. Conversion values and enantiomeric excess of products were similar to those registered at analytical scale, with good isolation yields and high optical purities (**Table II.3**).

Table II.3. Preparative-scale production. Conversion and enantiomeric excess (*ee*) values obtained in the ammonia addition and elimination reactions under optimal conditions at 0.5-gram scale.

Reaction type	Product	Reaction time (h)	Y* (%)	*ee* (%)	$[\alpha]_D^{27}$ #	Use
Ammonia addition	(*S*)-**1e**	42	59	>99	-66.4	HIV protease inhibitors[35]
	(*S*)-**1i**	48	82	>99	-47.6	Sansamycin analogues[36], biarylalanines[34]
	(*S*)-**1k**	48	52	>99	-35.2	KIFC1 inhibitors[37]
Ammonia elimination	(*R*)-**1c**	30	49	95	+5.7	Pin1 inhibitors[38], formyl peptide receptor 1 antagonists[39]
	(*R*)-**1k**	30	39	93	+31.5	(*R*)-PFI-2[40]

*Y=the reaction yield determined from the preparative scale reaction including product isolation, purification steps; #the measurements were performed in MeOH with substrate concentration of 10 mg/mL.

II.3 Conclusions

The present study demonstrates the successful synthetic applicability of previously engineered *Pc*PAL mutants (L256V, L134A, I460V)[23] for the efficient biocatalytic synthesis of enantiopure L- and D-Phe derivatives of high industrial value. Optimal conditions for ammonia addition and elimination reactions were achieved through medium engineering. Ammonia addition reactions have notable advantages over ammonia elimination reactions in terms of synthetic potential. This is because they offer a 100% theoretical yield for L-Phe analogues and utilize synthetically accessible, achiral starting materials. In contrast, ammonia elimination reactions yield enantiomerically enriched D-phenylalanines with a maximum theoretical yield of 50%, which is achieved through a kinetic resolution process from racemic amino acid starting materials.

The final stationary conversions in ammonia addition reactions are significantly affected by substrate concentration, especially for substrates that contain *meta*-positioned groups or electron-withdrawing substituents such as -Br or -CF_3. Specific reaction conditions are necessary for each substrate in case of ammonia elimination reactions, including the use of different buffer systems as reaction media, varying pH values and adjusting the (OD: mM) ratio, as these factors can influence the conversion and enantiomeric excess values. However, it should be noted that high substrate concentrations can inhibit both ammonia addition and elimination reactions, resulting in reduced conversion and enantioselectivity in the resolution process.

CHAPTER III. Towards a general approach for tailoring the hydrophobic binding site of phenylalanine ammonia-lyases

III.1 Background (literature data)

III.2 Results and Discussion

The development of novel PALs from different origins is continuously expanding[23, 32, 33, 41]. The hydrophobic binding region responsible for the facile active site accommodation of the substrate's aromatic ring also shows high similarity, however in several cases polar residues also appear in PALs of different origin. A polar amino acid residue such as histidine at analogue position to 137 in *Pc*PAL provides also a TAL-activity (tyrosine ammonia-lyase). This is why PAL enzymes from *Rhodotorula glutinis* (*Rg*PAL) and *Rhodosporidium toruloides* (*Rt*PAL), have a reported PAL/TAL activity[42] and are capable of deamination/amination of aromatic amino acids phenylalanine and tyrosine. Sequence alignment of PALs of different origins revealed that *At*PAL is highly similar to *Pc*PAL sharing a sequence identity of 81%, whereas *Rt*PAL shares only a 38% sequence identity to *Pc*PAL, but an almost identical catalytical site with the exception of positions analogue to 137 and 138 of *Pc*PAL (**Table III.1**).

Table III.1. The amino acid residues of the hydrophobic and polar substrate binding region of *At*PAL and *Rt*PAL based on sequence alignment with *Pc*PAL. The amino acids residues subjected to mutations are marked with blue (*ortho*), orange (*meta*), green (*para*), while major differences between PALs are marked with red colour.

Enzyme	*Pc*PAL	*At*PAL	*Rt*PAL	Enzyme	*Pc*PAL	*At*PAL	*Rt*PAL
Hydrophobic binding pocket	L206	L207	L215	Polar region	Y110	Y109	Y110
	L256	**L257**	**L266**		N384	N385	N397
	V259	V260	V269		Q348	Q349	Q360
	L134	**L133**	**L134**		Y351	Y352	Y363
	L138	L137	**Q138**		N487	N488	N499
	F137	**F136**	**H137**		E484	E485	E496
	I460	**I461**	**I472**		K456	K457	K468
MIO	202-204	203-205	211-213		R354	R355	R366

III.2.1 Generating novel mutant PAL libraries

Individual mutation of residues L134, F137, L256 and I460 from the hydrophobic binding pocket of *Pc*PAL resulted in a focused PAL variant library with increased catalytic activity and selectivity towards monosubstituted phenylalanines and cinnamic acids with electron-donating and electron-withdrawing groups at all positions (*ortho*, *meta*, *para*) of their aromatic ring[23]. The same key amino acid residues that act as substrate specificity modulators were replaced in *At*PAL and *Rt*PAL obtaining eight new PAL variants (L257V, L133A, F136V, I461V *At*PAL and L266V, L134A, H137V, I472V *Rt*PAL) (**Figure III.1**). In initial activity screenings, the mutant variant H137V *Rt*PAL showed reduced biocatalytic activity contrary to its homologue F137V *Pc*PAL. The cause was presumably due to the presence of Q138 residue in its proximity with whom is involved in

creating of a H-bond network. Therefore, new *Rt*PAL mutants were designed by adapting the mutational strategy and creating a '*Pc*PAL-like' *Rt*PAL library that resemble more the catalytic site of *Pc*PAL: H137F/Q138L, H137F/Q138L/L266V, H137V/Q138L and H137F/Q138L/I472V homologues to *wild-type*, L256V, F137V and I460V *Pc*PAL, respectively. Unfortunately, we failed to obtain H137F/Q138L/L134A mutant through site-directed mutagenesis despite applying different protocol optimizations.

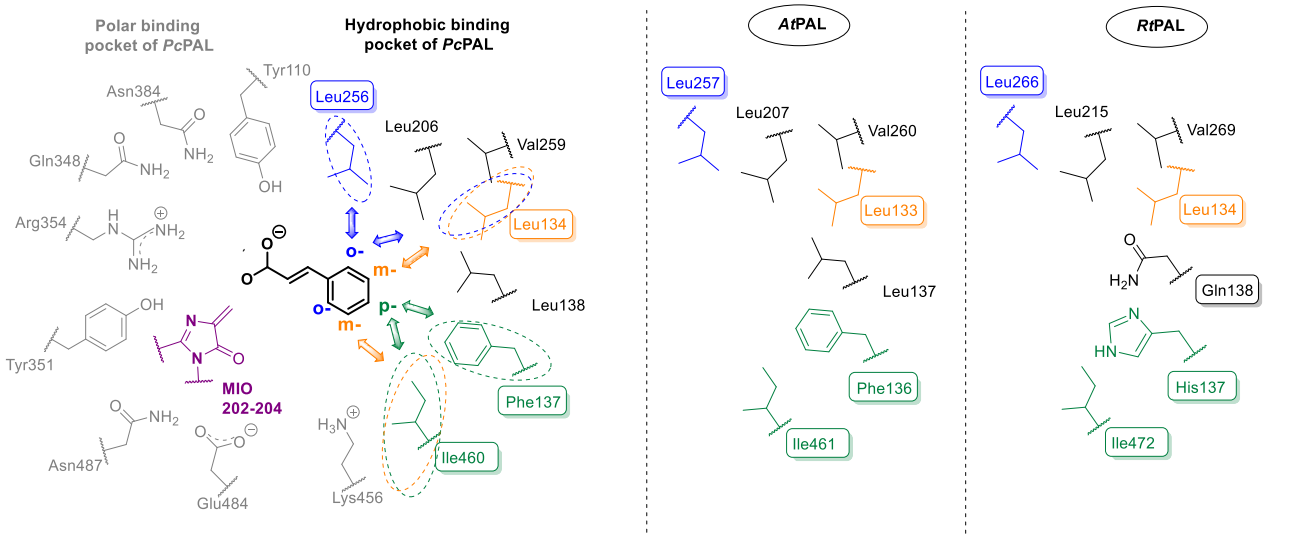

Figure III.1. Catalytic site model of *Pc*PAL[23] with bound *trans*-cinnamic acid. The interaction between the amino acid residues from the hydrophobic binding pocket and aryl ring substituents are marked with blue (*ortho*), orange (*meta*) and green (*para*). Homologue substrate specificity modulating amino acid residues in *At*PAL and *Rt*PAL are shown based on their sequence alignment with *Pc*PAL. Residues placed in boxes were replaced with alanine or valine for accommodation of ring substituents.

III.2.2 Substrate scope profiling

The activity of new *At*PAL and *Rt*PAL mutants was characterized through conversion values of the ammonia addition and elimination reaction of monosubstituted phenylalanine and cinnamic acid derivatives, *rac*-**1a-l** and **2a-l**, respectively (**Figure III.2**). Moreover, in case of deamination reactions, kinetic parameters (K_M, k_{cat} and k_{cat}/K_M) were also determined in order to give a better insight about the effect of homologue mutations upon the catalytic performance of PAL enzymes of different origin. The previously reported *Pc*PAL single mutants[23] with the highest conversion and relative activities in both ammonia addition and ammonia elimination reactions of ring-substituted substrates *rac*-**1a-l** and **2a-l** were used as comparison term.

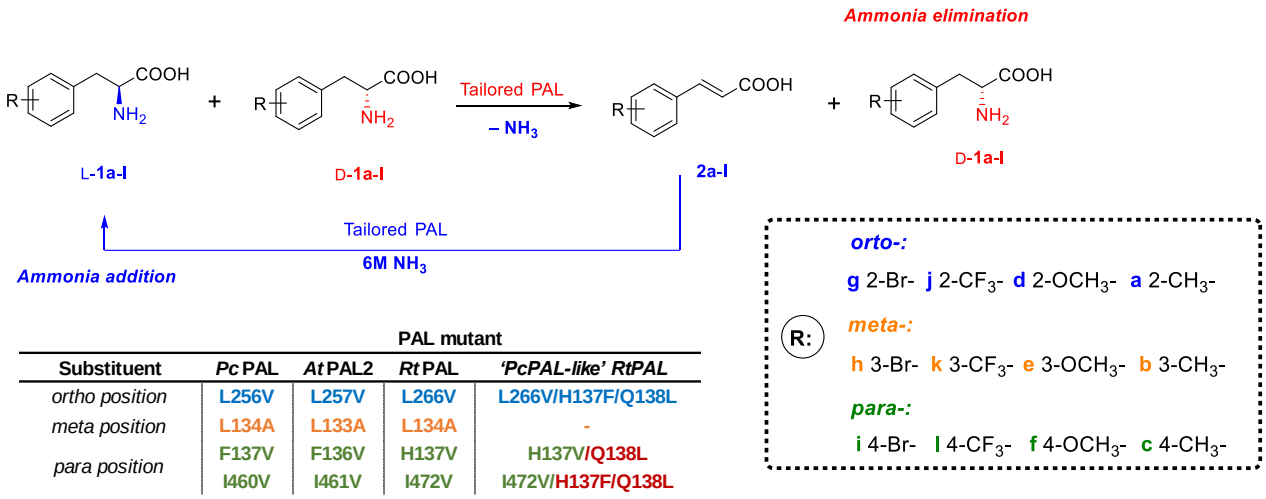

	PAL mutant			
Substituent	*Pc* PAL	*At* PAL2	*Rt* PAL	*'PcPAL-like' RtPAL*
ortho position	L256V	L257V	L266V	L266V/H137F/Q138L
meta position	L134A	L133A	L134A	-
para position	F137V	F136V	H137V	H137V/Q138L
	I460V	I461V	I472V	I472V/H137F/Q138L

Figure III.2. PAL-mediated ammonia elimination and ammonia addition reactions of ring-substituted *rac*-**1a-l** and **2a-l**.

III.2.2.1 Case 1: Substrates with an ortho-substituted phenyl ring

Whole-cell PAL-mediated biotransformations of *ortho*-substituted substrates showed that *At*PAL variants had higher conversion values compared to *Pc*PAL variants, and even the *wild-type At*PAL performed better than the *wild-type Pc*PAL in both ammonia addition and ammonia elimination reactions of **2a**,**d**,**g**,**j** and *rac*-**1a**,**d**,**g**,**j**, respectively. Notably, in the amination of substrates with electron donor *o*-OCH_3 and *o*-CH_3 substituents of high synthetic interest, *wild-type At*PAL showed significantly higher conversion values compared to *wild-type Pc*PAL. In contrast, *wild-type* RtPAL underperformed in both reaction routes. Furthermore, the mutation of *At*PAL and *Pc*PAL variants led to enhanced conversion-based enzyme activity, with *At*PAL variants L257V and L133A showing higher catalytic efficiencies than the corresponding *Pc*PAL variants L256V and L134A, as indicated by conversion and k_{cat} values (**Table III.2**).

In experiments using *wild-type At*PAL and mutant variant L257V, both substrates *o*-Br-cinnamic acid **2g** and *o*-Br-phenylalanine *rac*-**1g** showed high stationary conversions of 94.3% and 47.6%, respectively, with only 1 hour of reaction time for ammonia addition and 6 hours for ammonia elimination. However, the higher k_{cat} value of L257V (0.435) compared to *wild-type At*PAL (0.210) suggests that the mutation increased catalytic efficiency. Similar results were observed for *o*-CF_3 substituted substrates **2j** and *rac*-**1j**, with L257V showing a 5.5-fold increase in k_{cat} value compared to the wild-type variant. *Wild-type Pc*PAL also performed well with these substrates, showing high conversions of 86.6% (for **2g** after 6 hours) and 75.4% (for **2j** after 6 hours), and the L256V variant showed moderately improved conversions. However, in the case of *o*-CF_3-phenylalanine, all mutant PALs showed decreased substrate affinity compared to their *wild-type* variants, as indicated by high K_M values, suggesting a less favorable accommodation of the substrate within the modified catalytic site.

The beneficial effect of analogue mutation L266V *Rt*PAL was also confirmed, by the higher conversions in the ammonia addition of **2g** (c_{2g}=94.2% after 6 h) and **2j** (c_{2j}=82.2% after 24 h) than those provided by *wild-type Rt*PAL, while triple mutant H137F/Q138L/L266V *Rt*PAL did not provide significant improvement in terms of conversions (**Table III.2**).

While *o*-OCH_3-substituted substrates were poorly transformed by all *Rt*PAL enzymes, reflected also in the high K_M values and negligible enhancement of k_{cat} by L134A mutant, *At*PAL L133A

provided a significantly increased conversion as high as 95.5% in ammonia addition of **2d** and a 3.5-fold increase in catalytic efficiency (k_{cat}). Computational studies suggest that the increased hydrophobicity in the region of residues H137F and Q138L is favorable for accommodating and transforming the substrate due to the position of the methyl group in proximity to both residues L134 and L266 (**Figure III.3**). In case of ammonia elimination from *rac*-*o*-CH_3-phenylalanine *rac*-**1a**, less significant improvement of k_{cat} and K_M values for L266V *Rt*PAL, L256V *Pc*PAL and L257V *At*PAL compared to the corresponding *wild-type* variants, resulting in comparable specificity constants.

Table III.2. Ammonia addition and ammonia elimination reactions of *ortho*-substituted cinnamic acids **2g,j,a,d** and *rac*-phenylalanines *rac*-**1g,j,a,d** respectively, catalyzed by different PAL variants.

Enzyme		***Pc*PAL**		***At*PAL**		***Rt*PAL**		
Variant		***wild-type***	**L256V**	***wild-type***	**L257V**	***wild-type***	**L266V**	**H137F/Q138L/L266V**
Substrate		*o*-Br/ *rac*-**1g, 2g**						
Ammonia addition[#] (c%, reaction time)		86.6 (6 h) 95.7 (24 h)	89.6 (6 h) 95.7 (24 h)	88.6 (0.5 h) 94.3 (1 h)	82.1 (0.5 h) 92.7 (1 h)	4.2 (1 h) 29.6 (6 h)	55.0 (1 h) 94.2 (6 h)	49.7 (1 h) 94.3 (6 h)
Ammonia elimination (c%, reaction time)		31.9 (6 h) 42.4 (24 h)	45.9 (6 h) 50.6 (24 h)	36.7 (3 h) 47.6 (6 h)	48.6 (3 h) 50.3 (6 h)	13.5 (6 h) 23.9 (24 h)	19.5 (6 h) 41.3 (24 h)	24.9 (6 h) 42.4 (24 h)
Kinetic parameters	**K_M (µM)**	153	110	199	184	662	254	59
	k_{cat} (s^{-1})	0.157	0.365	0.210	0.435	0.094	0.079	0.046
	k_{cat}/K_M ($s^{-1}/µM^{-1}$)	$1.02 \cdot 10^{-3}$	$3.31 \cdot 10^{-3}$	$1.05 \cdot 10^{-3}$	$2.36 \cdot 10^{-3}$	$1.42 \cdot 10^{-4}$	$3.11 \cdot 10^{-4}$	$7.78 \cdot 10^{-4}$
Enzyme		***Pc*PAL**		***At*PAL**		***Rt*PAL**		
Variant		***wild-type***	**L256V**	***wild-type***	**L257V**	***wild-type***	**L266V**	**H137F/Q138L/L266V**
Substrate		*o*-CF_3/ *rac*-**1j, 2j**						
Ammonia addition[#] (c%, reaction time)		31.2 (3 h) 75.4 (24 h)	35.2 (3 h) 83.8 (24 h)	41.4 (0.5 h) 86.2 (3 h)	51.1 (0.5 h) 83.7 (3 h)	9.0 (6 h) 34.8 (24 h)	69.2 (6 h) 82.2 (24 h)	69.6 (6 h) 83.2 (24 h)
Ammonia elimination (c%, reaction time)		37.5 (6 h) 49.7 (24 h)	49.8 (6 h) 50.2 (24 h)	37.1 (0.5 h)	50.6 (0.5 h)	24.7 (6 h)	34.8 (6 h)	43.9 (6 h)
Kinetic parameters	**K_M (µM)**	523	2733	240	2911	92	1225	103
	k_{cat} (s^{-1})	0.042	0.148	0.032	0.177	0.004	0.019	0.117
	k_{cat}/K_M ($s^{-1}/µM^{-1}$)	$8.03 \cdot 10^{-5}$	$5.41 \cdot 10^{-5}$	$1.33 \cdot 10^{-4}$	$6.08 \cdot 10^{-5}$	$4.34 \cdot 10^{-5}$	$1.55 \cdot 10^{-5}$	$1.14 \cdot 10^{-3}$
Enzyme		***Pc*PAL**		***At*PAL**		***Rt*PAL**		
Variant		***wt***	**L134A**	***wt***	**L134A**	***wt***	**L134A**	**H137F/Q138L/L266V**
Substrate		*o*-OCH_3/ *rac*-**1d, 2d**						
Ammonia addition[#] (c%, reaction time)		5.5 (24 h)	40.8 (24 h)	19.3 (24 h)	95.5 (24 h)	<1 (16 h)	2.7 (16 h)	17.4 (16 h)
Ammonia elimination (c%, reaction time)		<1 (24 h)	15.6 (24 h)	6.4 (16 h)	45.2 (16 h)	3.1 (16 h)	<1 (16 h)	19.3 (16 h)
Kinetic parameters	**K_M (µM)**	3351	403	4752	326	2580	6552	n.d.
	k_{cat} (s^{-1})	0.019	0.134	0.019	0.058	0.014	0.016	n.d.

	k_{cat}/K_M ($s^{-1}/\mu M^{-1}$)	$5.67 \cdot 10^{-6}$	$3.32 \cdot 10^{-4}$	$3.99 \cdot 10^{-6}$	$1.78 \cdot 10^{-4}$	$5.43 \cdot 10^{-6}$	$2.44 \cdot 10^{-6}$	n.d.
Enzyme		***Pc*PAL**		***At*PAL**		***Rt*PAL**		
Variant		***wt***	**L256V**	***wt***	**L257V**	***wt***	**L266V**	**H137F/Q138L/L266V**
Substrate		*o*-CH_3/ *rac*-**1a, 2a**						
Ammonia addition# (c%, reaction time)		61.7 (6 h) 75.8 (24 h)	42.9 (6 h) 74.1 (24 h)	53.8 (1 h) 83.0 (3 h)	54.9 (1 h) 83.5 (3 h)	30.4 (3 h) 78.5 (24 h)	55.3 (3 h) 85.7 (24 h)	60.7 (3 h) 86.6 (24 h)
Ammonia elimination (c%, reaction time)		34.4 (6 h)	35.0 (6 h)	32.9 (1 h) 48.8 (6 h)	36.1 (1 h) 47.7 (6 h)	29.5 (6 h)	27.3 (6 h)	20.7 (6 h)
Kinetic parameters	K_M (μM)	59	128	46	n.d.	663	760	96
	k_{cat} (s^{-1})	0.211	0.282	0.119	0.226	0.252	0.268	0.115
	k_{cat}/K_M ($s^{-1}/\mu M^{-1}$)	$3.58 \cdot 10^{-3}$	$2.20 \cdot 10^{-3}$	$2.58 \cdot 10^{-3}$	n.d.	$3.80 \cdot 10^{-4}$	$3.53 \cdot 10^{-4}$	$1.19 \cdot 10^{-3}$

n.d. – not determinable, during enzyme kinetics the non-linear range of the Michaelis-Menten curve was not obtained using substrate concentration allowed by the solubility of the tested compounds. # ee_L>99% in the ammonia additions reactions

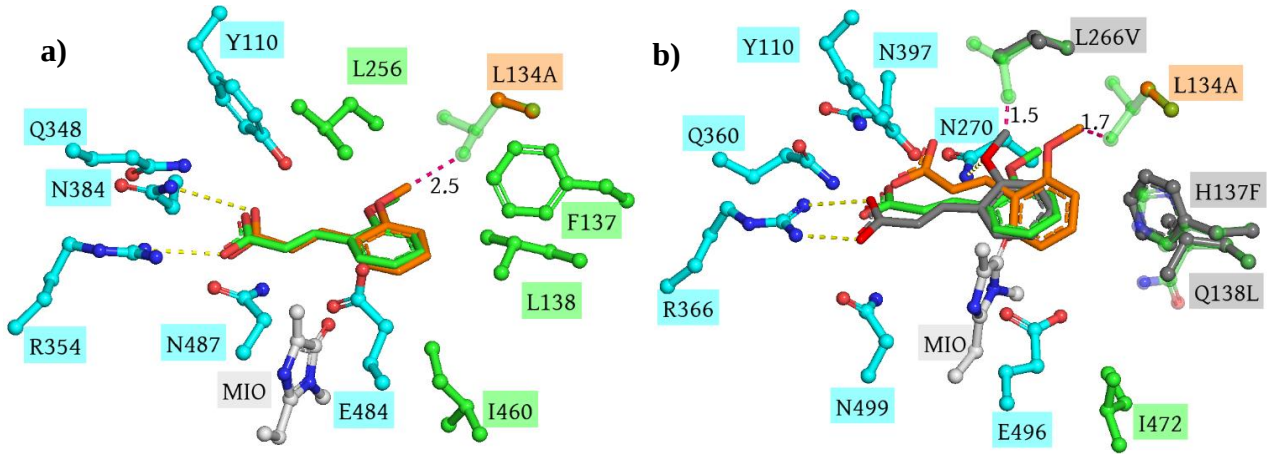

Figure III.3. Flexible and rigid molecular docking of *o*-OCH_3-cinnamic acid **2d**: **a)** catalytic site of *wild-type Pc*PAL (green, -7.3 kcal/mol) and L134A *Pc*PAL (orange, -7.7 kcal/mol); **b)** catalytic site of *wild-type Rt*PAL (green, -4.2 kcal/mol), L134A *Rt*PAL (orange, -6.9 kcal/mol) and H137F/Q138L/L266V *Rt*PAL (grey, -8 kcal/mol). Steric clashes between the *o*-OCH_3 substituent and side chains of residues L266, L134 in *Rt*PAL and L134 in *Pc*PAL are marked with pink dashed lines.

III.2.2.2 Case 2: Substrates with a meta-substituted phenyl ring

For *meta*-series of substituted cinnamic acids **2h,k,b** and *rac*-phenylalanines *rac*-**1h,k,b,** an increased catalytic performance was observed with *wild-type Rt*PAL in comparison with *wt-Pc*PAL and *wt-At*PAL, supported by higher k_{cat} values and conversion values (**Table III.3**). *m*-OCH3-substituted substrates **2e** and *rac*-**1e** were best transformed by L133A variant of *At*PAL, with 87.0% conversion in ammonia addition and 49.1% conversion in ammonia elimination. Similar values were obtained with *Pc*PAL L134A mutant ($c_{addition}$=74.8% and $c_{elimination}$=47.7% after 24 h) while for *Rt*PAL, the equivalent mutation did not improve the conversion. The same conversion trend was observed for all three PAL enzymes for *m*-CH3-substituted substrates.

The inferior catalytic performance registered with I472V *Rt*PAL, as well as with "*Pc*PAL-like" I472V/H137F/Q138L *Rt*PAL variant, is likely due to the presence of polar residues at positions 137 (histidine) and 138 (glutamine), which play a role in accommodation of substrates bearing

electron withdrawing groups (-Br, -CF_3) as substituents. Molecular docking suggests that the presence of polar residues Q138 and H137 somewhat shifts the orientation of *meta*-substituents within the catalytic site from the predicted and previously explored positions in case of *Pc*PAL towards L134 residue. This is supported by the experimental results, where L134A variant provided conversion and kinetic data that were more in line with those observed for *wt-Rt*PAL for all tested substrates. Unfortunately, the unsuccessful site-directed mutagenesis for "*Pc*PAL-like" L134A/H137F/Q138L variant didn't allow testing the combined effect of replacing polar amino acid residues H137, Q138, and L134 (**Figure III.4**).

Table III.3. Ammonia addition and ammonia elimination reactions of *meta*-substituted cinnamic acids **2h,k,e,b** and *rac*-phenylalanines *rac*-**1 h,k,e,b** respectively, catalyzed by different PAL variants.

Enzyme	***Pc*PAL**			***At*PAL**			***Rt*PAL**			
Variant	***wild-type***	**I460V**	**L134A**	***wild-type***	**I461V**	**L133A**	***wild-type***	**I472V**	**L134A**	**H137F/Q138L/I472V**
Substrate	*m*-Br/ *rac*-**1h, 2h**									
Ammonia addition[#] (c%, reaction time)	36.1 (3 h) 84.4 (24 h)	51.7 (3 h) 90.8 (24 h)	51.4 (3 h) 89.6 (24 h)	24.2 (0.5 h) 77.9 (3 h)	76.5 (0.5 h) 87.3 (3 h)	74.6 (0.5 h) 87.5 (3 h)*	65.6 (3 h) 83.8 (6 h)	11.7 (6 h) 39.1 (24 h)	73.3 (3 h) 88.2 (6 h)	<1 (6 h) 4.1 (24 h)
Ammonia elimination (c%, reaction time)	31.8 (6 h)	30.4 (6 h)	37.2 (6 h)	33.6 (1 h)	26.6 (1 h)	47.7 (1 h)	40.0 (3 h)	31.9 (24 h)	37.1 (3 h)	<1 (24 h)
Kinetic parameters K_M (μM)	153	51	-	n.d.	55	76	363	n.d.	409	n.d.
Kinetic parameters k_{cat} (s^{-1})	0.095	0.154	-	0.07	0.197	0.395	0.343	n.d.	0.288	n.d.
Kinetic parameters k_{cat}/K_M ($s^{-1}/\mu M^{-1}$)	$6.21 \cdot 10^{-4}$	$3.02 \cdot 10^{-3}$	-	n.d.	$3.58 \cdot 10^{-3}$	$5.19 \cdot 10^{-3}$	$9.45 \cdot 10^{-4}$	n.d.	$7.04 \cdot 10^{-4}$	n.d.
Enzyme	***Pc*PAL**			***At*PAL**			***Rt*PAL**			
Variant	***wild-type***	**I460V**	**L134A**	***wild-type***	**I461V**	**L133A**	***wild-type***	**I472V**	**L134A**	**H137F/Q138L/I472V**
Substrate	*m*-CF_3/ *rac*-**1k, 2k**									
Ammonia addition[#] (c%, reaction time)	1.8 (6 h) 20.2 (24 h)	33.5 (6 h) 66.9 (24 h)	8.9 (6 h) 12.7 (24 h)	6.0 (6 h) 18.4 (24 h)	73.6 (6 h) 86.6 (24 h)	17.1 (6 h) 23.8 (16 h)	18.0 (6 h) 40.2 (24 h)	<1 (6 h) 7.3 (24 h)	16.0 (6 h) 52.6 (24 h)	<1 (6 h) <1 (24 h)
Ammonia elimination (c%, reaction time)	2.2 (6 h) 7.4 (24 h)	26.1 (6 h) 46.6 (24 h)	19.9 (6 h) 44.0 (24 h)	13.4 (3 h)	50.4 (3 h)	35.5 (3 h)	34.1 (6 h)	4.8 (24 h)	26.1 (6 h)	<1 (24 h)
Kinetic parameters K_M (μM)	533	163	912	217	112	-	1369	2505	1573	-
Kinetic parameters k_{cat} (s^{-1})	0.057	0.2	0.203	0.04	0.272	-	0.11	0.013	0.085	-
Kinetic parameters k_{cat}/K_M ($s^{-1}/\mu M^{-1}$)	$1.07 \cdot 10^{-4}$	$1.23 \cdot 10^{-3}$	$2.23 \cdot 10^{-4}$	$1.84 \cdot 10^{-4}$	$2.43 \cdot 10^{-3}$	-	$8.03 \cdot 10^{-5}$	$5.19 \cdot 10^{-6}$	$5.40 \cdot 10^{-5}$	-
Enzyme	***Pc*PAL**			***At*PAL**			***Rt*PAL**			
Variant	***wild-type***		**L134A**	***wild-type***		**L134A**	***wild-type***		**L134A**	
Substrate	*m*-OCH_3/ *rac*-**1e, 2e**									
Ammonia addition[#] (c%, reaction time)	5.9 (3 h) 31.9 (24 h)		42.0 (3 h) 74.8 (24 h)	11.0 (6 h) 52.1 (24 h)		87.0 (3 h) 87.7 (24 h)	17.5 (24 h)		14.0 (24 h)	

Ammonia elimination (c%, reaction time)		18.9 (24 h)	47.7 (24 h)	47.0 (24 h)	49.1 (24 h)	22.6 (16 h)	33.3 (16 h)
Kinetic parameters	**K_M (μM)**	378	170	297	49	2971	4291
	k_{cat} (s^{-1})	0.011	0.431	0.095	0.213	0.078	0.07
	k_{cat}/K_M ($s^{-1}/\mu M^{-1}$)	$2.91 \cdot 10^{-5}$	$2.53 \cdot 10^{-3}$	$3.19 \cdot 10^{-4}$	$4.35 \cdot 10^{-3}$	$2.62 \cdot 10^{-5}$	$1.63 \cdot 10^{-5}$
Enzyme		***Pc*PAL**		***At*PAL**		***Rt*PAL**	
Variant		***wild-type***	**L134A**	***wild-type***	**L134A**	***wild-type***	**L134A**
Substrate		*m*-CH_3/ *rac*-**1b, 2b**					
Ammonia addition# (c%, reaction time)		2.3 (24 h)	26.4 (24 h)	7.4 (6 h) 23.7 (16 h)	74.8 (3 h) 80.2 (24 h)	25.7 (16 h)	29.1 (16 h)
Ammonia elimination (c%, reaction time)		10.8 (24 h)	28.9 (24 h)	22.9 (6 h)	45.5 (6 h)	45.0 (16 h)	50.5 (16 h)
Kinetic parameters	**K_M (μM)**	55	115	n.a.	63	333	338
	k_{cat} (s^{-1})	0.014	0.1	n.a.	0.113	0.153	0.146
	k_{cat}/K_M ($s^{-1}/\mu M^{-1}$)	$2.54 \cdot 10^{-4}$	$8.69 \cdot 10^{-4}$	n.a.	$1.79 \cdot 10^{-3}$	$4.59 \cdot 10^{-4}$	$4.32 \cdot 10^{-4}$

n.d. – not determinable, during enzyme kinetics the non-linear range of the Michaelis-Menten curve was not obtained using substrate concentration allowed by the solubility of the tested compounds; **n.a.** – no activity detected; "**-**"– no measurement was performed

ee_L >99% in the ammonia additions reactions, except in case of the L-**1h** (*ee* = 93.6%) produced within the ammonia addition reaction of **2h** catalyzed by L134A *At*PAL

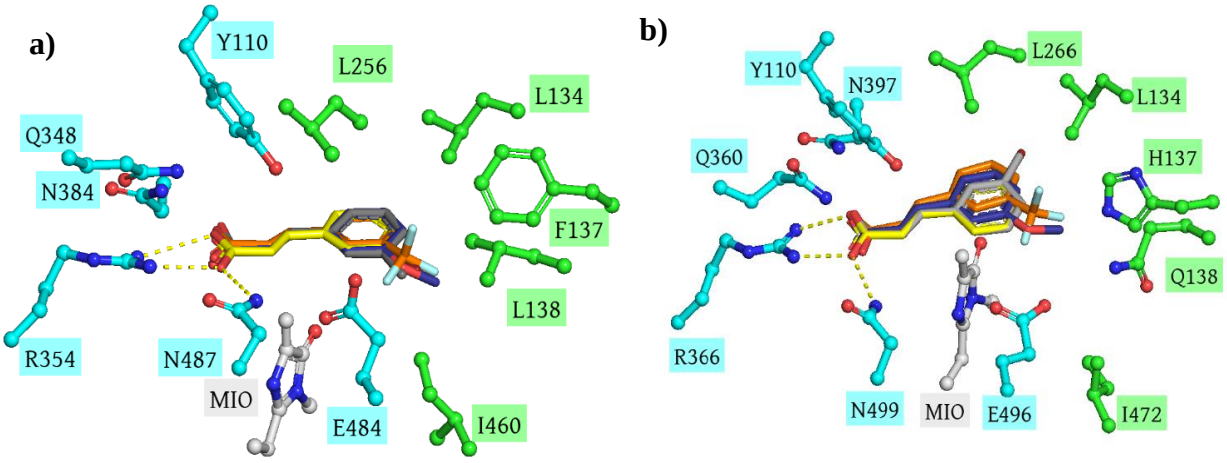

Figure III.4. Accommodation of *meta-substituted* substrates *m*-Br-cinnamic acid **2h** (yellow), *m*-CF_3-cinnamic acid **2k** (orange), *m*-OCH_3-cinnamic acid **2e** (blue) and *m*-CH_3-cinnamic acid **2b** (grey) within the catalytic site of **a)** *wild-type Pc*PAL and **b)** *wild-type Rt*PAL. Residues from the hydrophobic binding region are marked in green, while residues from the polar binding region are marked in cyan.

III.2.2.3 Case 3: Substrates with para-substituted phenyl ring

The low conversions obtained with *wild-type Pc*PAL in the case of *p*-substituted substrates (**Table III.4**) is believed to be due to the steric clash between the *p*-substituent and active site residues, as described in our previous report[23]. This proved to be true in case of *wild-type Rt*PAL, but not *wild-type At*PAL, although the later has an 81% sequence identity when compared to PAL from *Petroselinum crispum*. The *wild-type At*PAL provided maximum conversion value in case of ammonia elimination of *p*-Br- and *p*-CH_3-phenylalanines *rac*-**1i,c** (c~50% after 6 and 16 h, respectively) and moderate conversion in case of *p*-CF_3-phenylalanines *rac*-**1l** (c=40% after 6 h). In

case of *p*-OCH_3-substituted substrates *wt-Pc/Rt*PALs proved to be inefficient, while *wt-At*PAL registered a similar behavior ($c_{rac\text{-}\mathbf{1f}}$=14% and $c_{\mathbf{2f}}$<1%).

The I461V and F136V *At*PAL mutants showed high conversion values, showing increased kinetic parameters in ammonia elimination reactions (16-fold increase in k_{cat} compared to *wt-At*PAL) (**Table III.4**). However, F136V *At*PAL, like its homologue in *Pc*PAL, affected the enantioselectivity of the amination reactions. The I461V *At*PAL-based biotransformation produced higher *ee* values compared to F136V *At*PAL.

Generally, *wild-type Rt*PAL has been shown to be ineffective in transforming *para*-substituted substrates, and mutations such as I472V or "*Pc*PAL-like" H137V/Q138L/I472V *Rt*PAL did not improve catalytic performance, similar to what was observed with meta-substituted substrates. The presence of polar residue Gln at position 138, close to V137, may be responsible for the poor catalytic performance of H137V. However, the H137V/Q138L *Rt*PAL variant showed enhanced catalytic efficiency towards all substrates compared to the single mutant variant H137V, and the conversion values were similar to those observed with *At*PAL and *Pc*PAL equivalents. Experimental data was supported by computational results, indicating a better accommodation of *para*-substituted substrates within the catalytic site of H137V/Q138L mutant compared to *wild-type Rt*PAL (**Figure III.5**)

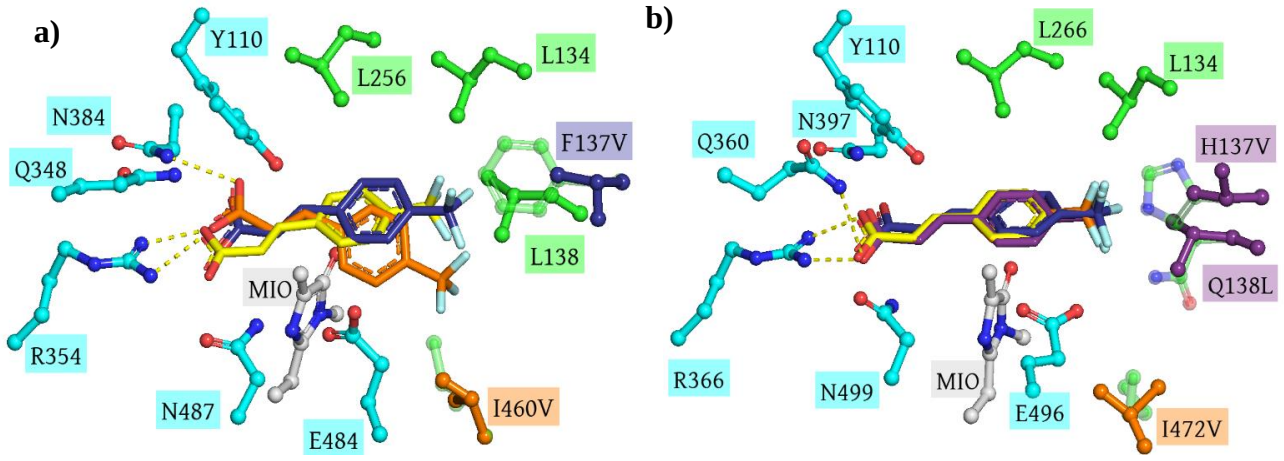

Figure III.5. Accommodation of *para-substituted* substrate *m*-CF_3-cinnamic acid **2k** within the catalytic site of **a)** *wild-type Pc*PAL and **b)** *wild-type Rt*PAL, with active orientation marked with yellow for *wt*-PcPAL (-4.8 kcal/mol) and *wt-Rt*PAL (-5.5 kcal/mol), orange for I460V *Pc*PAL (-6.4 kcal/mol) and I472V *Rt*PAL (-5.5 kcal/mol), blue for F137V *Pc*PAL (-8.9 kcal/mol) and H137V *Rt*PAL (-6.9 kcal/mol), purple for H137V/Q138L *Rt*PAL (-7.5 kcal/mol). Residues from the hydrophobic binding region are marked in green, while residues from the polar binding region are marked in cyan.

Table III.5. Ammonia addition and ammonia elimination reactions of *para*-substituted cinnamic acids **2i,l,f,c** and *rac*-phenylalanines *rac*-**1i,l,f,c** respectively, catalyzed by different PAL variants.

Enzyme	***Pc*PAL**			***At*PAL**			***Rt*PAL**				
Variant	***wild-type***	**I460V**	**F137V**	***wild-type***	**I461V**	**F136V**	***wild-type***	**I472V**	**H137V**	**H137F/ Q138L/ I472V**	**H137V/ Q138L**
Substrate	*p*-Br/ *rac*-**1i, 2i**										
Ammonia addition[#] (c%, reaction time)	7.1 (24 h)	58.8 (24 h)	71.6 (24 h)*	84.7 (16 h)	90.5 (16 h)	89.4 (16 h)*	<1 (16 h)	<1 (16 h)	18.5 (16 h)	<1 (16 h)	84.3 (16 h)

Ammonia elimination (c%, reaction time)		49.9 (24 h)	51.5 (24 h)	59.8 (24 h)**	51.5 (6 h)	53.4 (6 h)	61.8 (6 h)**	<1 (16 h)	<1 (16 h)	23.1 (16 h)	<1 (16 h)	50.3 (16 h)
Kinetic parameters	**K_M (µM)**	269	71	-	73	61	-	621	2120	-	n.a.	n.a.
	k_{cat} (s^{-1})	0.165	0.259	-	0.085	0.245	-	0.005	0.008	-	n.a.	n.a.
	k_{cat}/K_M ($s^{-1}/µM^{-1}$)	$6.13\cdot10^{-4}$	$3.65\cdot10^{-3}$	-	$1.16\cdot10^{-3}$	$4.01\cdot10^{-3}$	-	$8.05\cdot10^{-6}$	$3.77\cdot10^{-6}$	-	n.a.	n.a.
Enzyme		***Pc*PAL**			***At*PAL**			***Rt*PAL**				
Variant		***wild-type***	**I460V**	**F137V**	***wild-type***	**I461V**	**F136V**	***wild-type***	**I472V**	**H137V**	**H137F/ Q138L/ I472V**	**H137V/ Q138L**
Substrate		*p*-CF_3/ *rac*-**1l, 2l**										
Ammonia addition[#] (c%, reaction time)		5.7 (16 h)	32.0 (6 h) 62.5 (24 h)	45.9 (3 h) 65.3 (24 h)*	48.9 (16 h)	36.1 (3 h) 88.7 (24 h)	92.8 (6 h) 93.8 (16 h)*	<1 (16 h)	<1 (16 h)	10.5 (16 h)	<1 (16 h)	82.8 (16 h)
Ammonia elimination (c%, reaction time)		9.3 (24 h)	37.3 (24 h)	50.2 (24 h)**	40.0 (6 h)	50.7 (6 h)	80.8 (6 h)**	<1 (16 h)	<1 (16 h)	7.9 (16 h)	<1 (16 h)	50.8 (16 h)
Kinetic parameters	**K_M (µM)**	2490	901	151	1467	275	-	6381	n.a.	3231	n.a.	n.a.
	k_{cat} (s^{-1})	0.25	0.55	0.42	0.127	0.428	-	0.004	n.a.	0.032	n.a.	n.a.
	k_{cat}/K_M ($s^{-1}/µM^{-1}$)	$1.00\cdot10^{-4}$	$6.10\cdot10^{-4}$	$2.78\cdot10^{-3}$	$8.66\cdot10^{-5}$	$1.55\cdot10^{-3}$	-	$6.27\cdot10^{-7}$	n.a.	$9.90\cdot10^{-4}$	n.a.	n.a.
Enzyme		***Pc*PAL**			***At*PAL**			***Rt*PAL**				
Variant		***wild-type***	**I460V**	**F137V**	***wild-type***	**I461V**	**F136V**	***wild-type***	**I472V**	**H137V**	**H137F/ Q138L/ I472V**	**H137V/ Q138L**
Substrate		*p*-OCH_3/ *rac*-**1f, 2f**										
Ammonia addition[#] (c%, reaction time)		<1 (24 h)	11.8 (24 h)	4.1 (24 h)	<1 (24 h)	24.5 (24 h)	23.7 (24 h)*	<1 (16 h)	<1 (16 h)	<1 (16 h)	<1 (16 h)	16.9 (16 h)
Ammonia elimination (c%, reaction time)		<1 (24 h)	17.0 (24 h)	15.4 (24 h)	14.1 (16 h)	42.0 (16 h)	38.4 (16 h)	<1 (16 h)	<1 (16 h)	<1 (16 h)	<1 (16 h)	25.3 (16 h)
Kinetic parameters	**K_M (µM)**	1858	265	-	1048	132	-	3219	n.d.	n.d.	-	-
	k_{cat} (s^{-1})	0.009	0.10	-	0.007	0.112	-	0.036	n.d.	n.d.	-	-
	k_{cat}/K_M ($s^{-1}/µM^{-1}$)	$4.84\cdot10^{-6}$	$3.88\cdot10^{-4}$	-	$6.68\cdot10^{-6}$	$8.48\cdot10^{-4}$	-	$1.12\cdot10^{-5}$	n.d.	n.d.	-	-
Enzyme		***Pc*PAL**			***At*PAL**			***Rt*PAL**				
Variant		***wild-type***	**I460V**	**F137V**	***wild-type***	**I461V**	**F136V**	***wild-type***	**I472V**	**H137V**	**H137F/ Q138L/ I472V**	**H137V/ Q138L**
Substrate		*p*-CH_3/ *rac*-**1c, 2c**										
Ammonia addition[#] (c%, reaction time)		1.7 (6 h) 4.0 (24 h)	13.5 (6 h) 34.1 (24 h)	16.6 (24 h)	3.8 (6 h) 13.3 (24 h)	28.6 (3 h) 54.6 (24 h)	29.2 (6 h) 33.3 (24 h)	<1 (16 h)	<1 (16 h)	<1 (16 h)	<1 (16 h)	61.0 (16 h)
Ammonia elimination (c%, reaction time)		6.0 (16 h)	10.7 (16 h)	22.1 (16 h)	50.0 (16 h)	50.1 (16 h)	36.2 (16 h)	<1 (16 h)	<1 (16 h)	<1 (16 h)	<1 (16 h)	9.6 (16 h)

Kinetic parameters	**K_M (µM)**	208	107	-	191	144	-	9902	n.a.	7080	n.a.	n.a.
	k_{cat} (s^{-1})	0.026	0.092	-	0.018	0.1	-	0.003	n.a.	0.003	n.a.	n.a.
	k_{cat}/K_M ($s^{-1}/\mu M^{-1}$)	$1.25 \cdot 10^{-4}$	$8.59 \cdot 10^{-4}$	-	$9.42 \cdot 10^{-5}$	$6.94 \cdot 10^{-4}$	-	$3.03 \cdot 10^{-7}$	n.a.	$4.24 \cdot 10^{-7}$	n.a.	n.a.

n.d. – not determinable, during enzyme kinetics the non-linear range of the Michaelis-Menten curve was not obtained using substrate concentration allowed by the solubility of the tested compounds; **n.a.** – no activity detected; "**-**" – no determination/measurement was performed;

ee_L>99% in the ammonia additions reactions, except in case of *** 1**. In case of **2i***: Pc*PAL F137V variant provided L-**1i** with *ee* = 97%; *At*PAL F136V variant provided L-**1i** with *ee* = 93%; **2**. in case of **2l**: *Pc*PAL F137V variant provided L-**1l** with *ee* = 82%; *At*PAL F136V variant provided L-**1l** with *ee* = 83 %; **3**. in case of **2f**: *At*PAL F136V variant provided L-**1f** with *ee* = 97 %; ****** during the kinetic resolution-type ammonia eliminations in case of high enantioselectivity the maximal conversion values of *rac*-phenylalanines is 50%, conversions exceeding this value, support the low enantioselectivity of the process

III.3 Conclusions

In this study, we aimed to develop a general rational design strategy for creating substrate-tailored PALs of various origins and substrate scopes. To achieve this, we utilized the mutational strategy developed for PAL from *Petroselinum crispum* on *At*PAL and *Rt*PAL, which are well-characterized PALs with different levels of sequence identity to *Pc*PAL. *Rt*PAL, which is known to have a dual PAL/TAL activity, showed distinct substrate specificity compared to *wt-Pc*/*At*PAL. The mutational strategy applied to *Rt*PAL, which included the replacement of residue Q138 near position 137 with hydrophobic residues, was found to significantly enhance the catalytic properties of H137V *Rt*PAL, making it a "*Pc*PAL like" variant. This supports the idea that further mutations can be made based on rational considerations to further improve the enzyme's properties. Within the generated mutant library of *At*PAL, *Rt*PAL and *Pc*PAL, the *At*PAL variants (with some exceptions) outperformed the corresponding *Pc*PAL homologues in terms of conversion and catalytic efficiency, even though they share a high level of identity of 81%.

The study demonstrates that mutational approaches can be used to enhance the catalytic efficiency of phenylalanine ammonia-lyases (PALs) variants towards non-natural substrates with different substitution patterns. The results suggest that this approach is applicable across PALs of different origins and can be further refined through sequence alignment-based rational modifications. Overall, the findings contribute to the development of a general rational design strategy for PAL (E.C. 4.3.1.24) and PAL/TAL classes (E.C. 4.3.1.25) and provides a foundation for future research in this area.

CHAPTER IV. Engineered, scalable production of optically pure L-phenylalanines using phenylalanine ammonia-lyase from *Arabidopsis thaliana*

IV.1 Background (literature data)

IV.2 Results and Discussion

Based on our recent work[43], we evaluated the improved catalytic efficiency of *At*PAL variants L257V, L133A and I461V in comparison with their *Pc*PAL homologues by conducting the amination of several monosubstituted cinnamic acids **2a-l**, under the same optimal conditions reported for *Pc*PAL-catalyzed ammonia additions[44] (**Figure IV.1**). Our assessment included monitoring the final stationary conversions and enantiomeric excess values of the products (L-**1a-l**), as well as the impact of substrate concentration on the conversion values, since substrate inhibition had previously been observed in some *Pc*PAL variants[44].

In our pursuit to develop an optimized preparative-scale biocatalytic process for the production of enantiopure unnatural amino acids of high industrial value, we evaluated the effect of several parameters on reaction time and conversion values. These parameters included the reaction medium/ammonia source, biocatalyst: substrate ratio, temperature, substrate concentration and the type of biocatalyst used. The goal was to identify the optimal conditions to achieve a highly improved and environmentally sustainable biotransformation process.

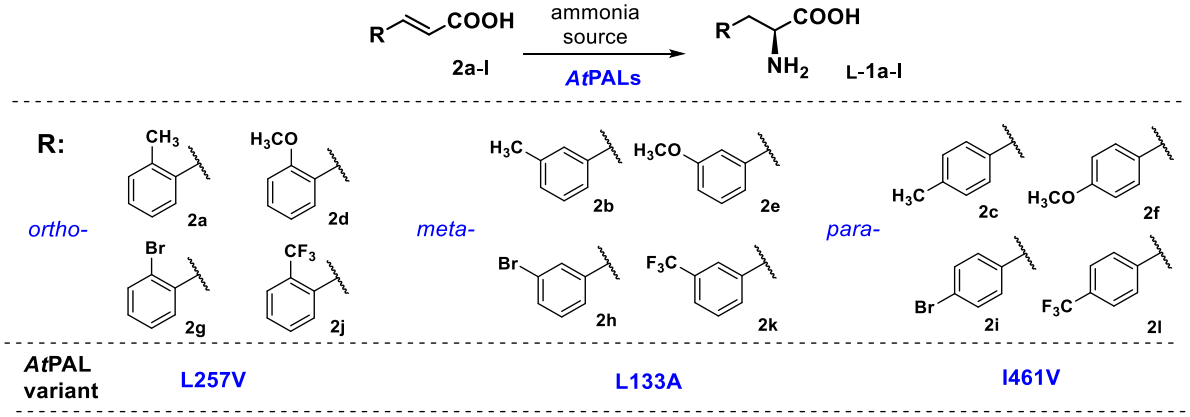

Figure IV.1. The *At*PAL-catalyzed ammonia addition reactions of cinnamic acids **2a-l** substituted in their *ortho-*, *meta-*, *para-* positions, subjected to the reaction engineering process.

IV.2.1 Optimization of *At*PAL-based amination reactions

IV.2.1.1 The effect of substrate concentration

The effect of substrate concentration on the catalytic performance of the engineered *At*PAL mutant variants (L133A, L257V and I461V) was tested in the ammonia addition onto all cinnamic acid analogues **2a-l** in the limit of their solubilities for 48 hours. Time conversion profiles are presented in **Figures IV.2-4**.

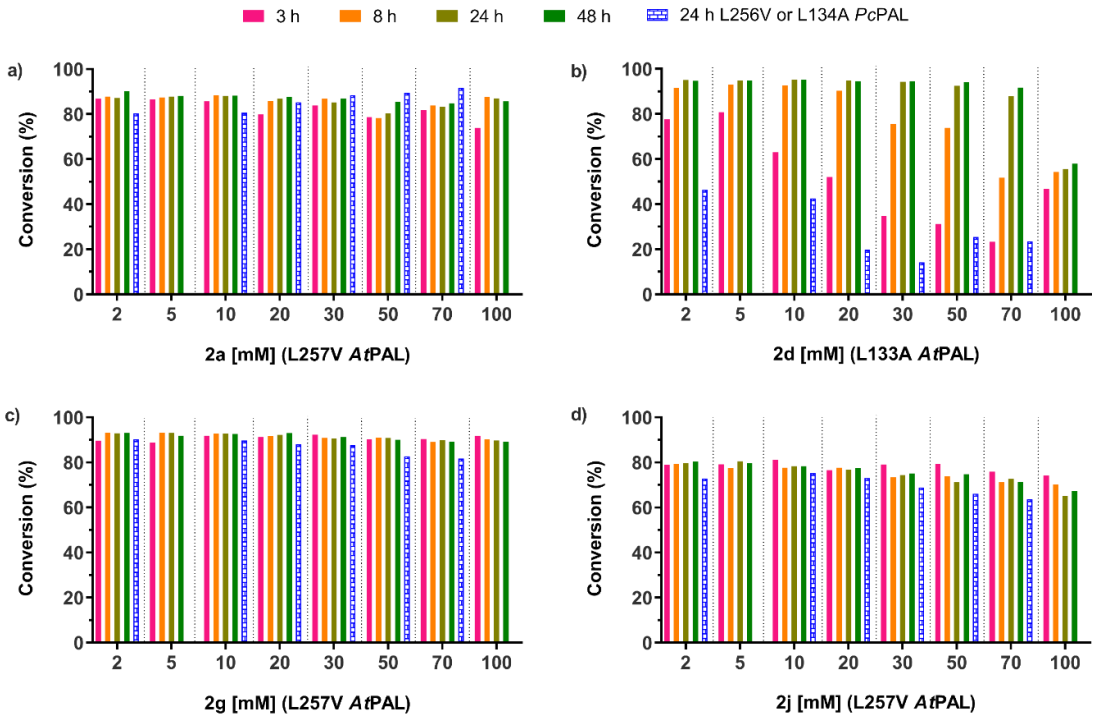

Figure IV.2. Time conversion profiles for the ammonia addition reactions onto a) *o*-CH_3-cinnamic acid **2a** b) *o*-OCH_3-cinnamic acid **2d** c) *o*-Br-cinnamic acid **2g** and d) *o*-CF_3-cinnamic acid **2j** using the corresponding *At*PAL variant. For comparison, conversion values given by the corresponding *Pc*PAL variant L256V or L134A after 24 h are marked with blue brick pattern .

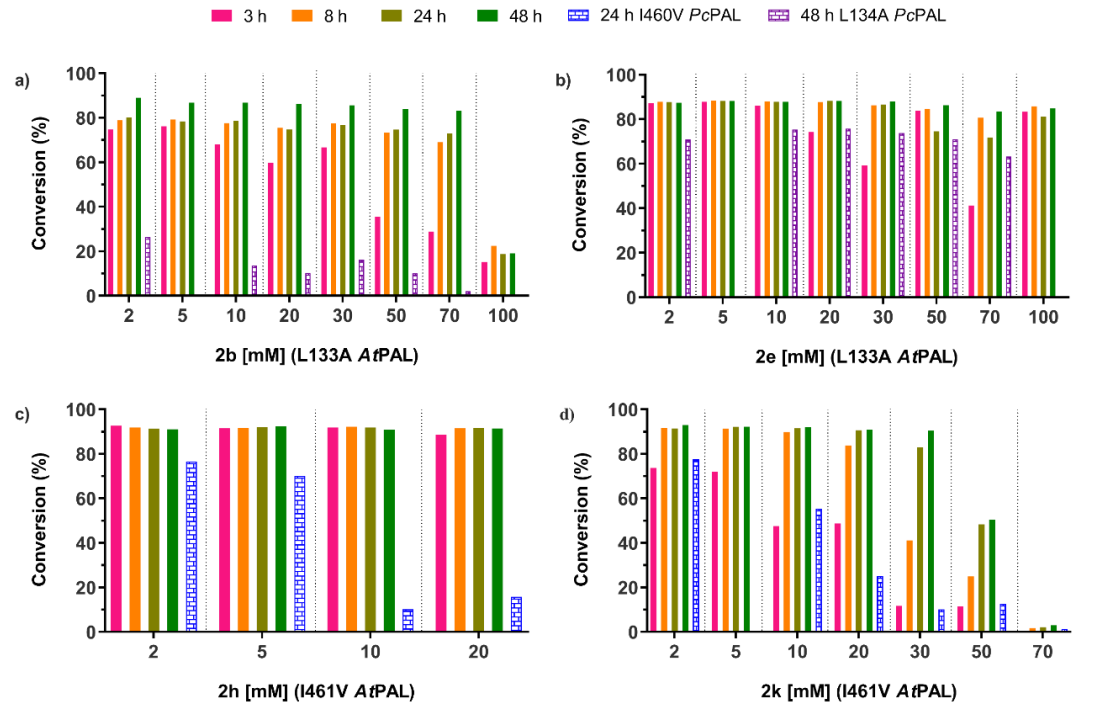

Figure IV.3. Time conversion profiles for the ammonia addition reactions onto a) *m*-CH_3-cinnamic acid **2b** b) *m*-OCH_3-cinnamic acid **2e** c) *m*-Br-cinnamic acid **2h** and d) *m*-CF_3-cinnamic acid **2k** using the corresponding *At*PAL variant. For comparison, conversion values given by the corresponding *Pc*PAL variants are marked with blue brick pattern (registered after 24 h using I460V mutant) and purple brick pattern (registered after 48 h using L134A mutant).

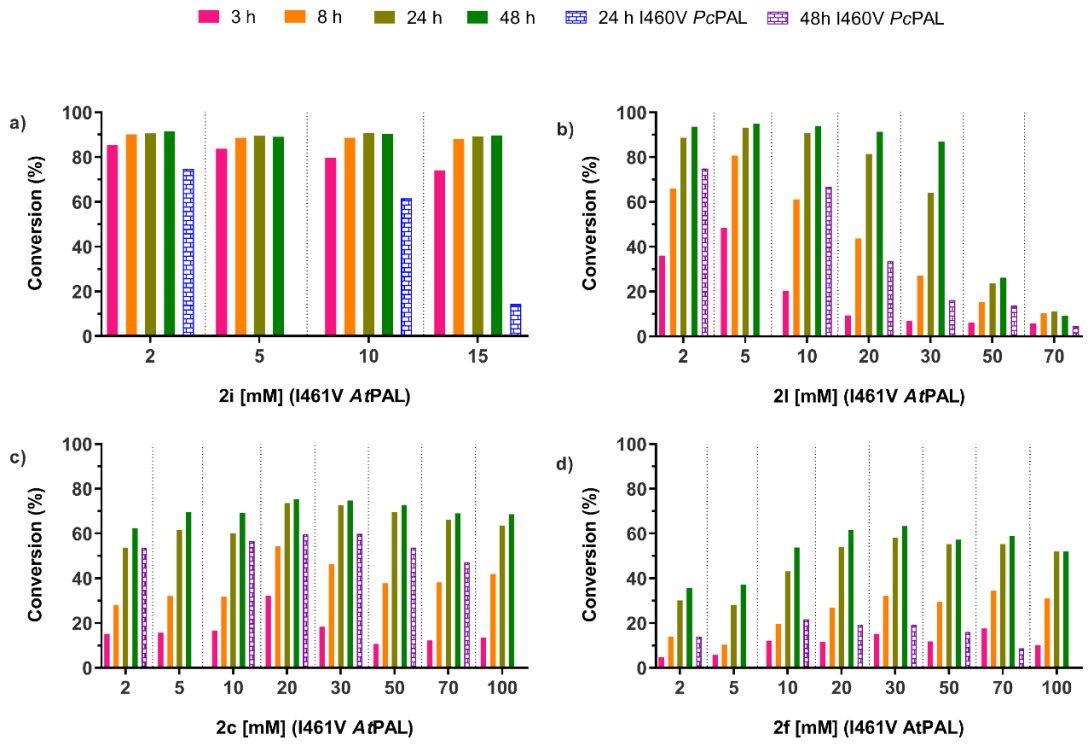

Figure IV.4. Time conversion profiles for the ammonia addition reactions onto a) *p*-CH_3-cinnamic acid **2c** b) *p*-OCH_3-cinnamic acid **2f** c) *p*-Br-cinnamic acid **2i** and d) *p*-CF_3-cinnamic acid **2l** using the corresponding *At*PAL variant. For comparison, conversion values given by the corresponding *Pc*PAL variants are marked with blue brick pattern (registered after 24 h using I460V mutant) and purple brick pattern (registered after 48 h using I460V mutant).

Our previous study[44] revealed that, as substrate concentrations increased, the reaction progression of *Pc*PAL variants L256V, L134A and I460V was significantly slowed (with some exceptions), implying the occurrence of substrate inhibition. On the other hand, the corresponding *At*PAL variants L257V, L133A and I461V exhibited robust performance, reaching high stationary conversions even at substrate concentrations close to the industrially relevant value of 100 mM (as illustrated in **Figures IV.2** through **IV.4**).

IV.2.1.1.1 AtPAL- versus PcPAL-based amination reactions of 2a-l

The ammonia addition reactions carried out with *At*PAL mutants resulted in high conversions and provided L-phenylalanine analogues L-**1a-l** in excellent enantiomeric excess values (ee_L) at significantly shorter reaction times compared to the ones observed in the case of *Pc*PAL variants-based amination reactions of the same substrates (**2a-l**) under the same optimal conditions. The optimal substrate concentrations were selected based on the shortest reaction time that led to the highest ee_L and conversion values (**Table IV.1**).

Previously reported[44] ammonia addition reactions of **2b** and **2f** using *Pc*PAL mutant variants registered low stationary conversions of 26.4% and 19.1%, respectively, while the use of *At*PAL mutants resulted in much higher conversions of 86.3% in case of **2b** and 63.4% in case of **2f**, after 48 h reaction time. Additionally, the *At*PAL variants L257V, L133A and I461V showed increased operational capability at significantly higher substrate concentrations in all cases compared to the corresponding *Pc*PAL homologues. The results obtained from the hydroamination reactions of

cinnamic acid derivatives **2a**, **2g**, **2j** and **2h** demonstrate the ability to reach maximal stationary conversion at high, 100 mM substrate concentrations (**Table IV.1**). This is a critical factor in terms of industrial feasibility and highlights the potential of this biocatalyst system in practical applications.

Table IV.1. Conversion and enantiomeric excess (ee_L) values obtained in the amination reactions of **2a-l** using *At*PAL variants. Comparative data registered using *Pc*PAL variants[44] is also presented.

Substrate	Substituent	*Pc*PAL variant	[S] (mM)	Time (h)	c (%)	ee_L (%)	*At*PAL variant	[S] (mM)	Time (h)	c (%)	ee_L (%)
2a	*o*-CH_3	L256V	70	24	91.5	>99	L257V	100	8	87.6	>99
2b	*m*-CH_3	L134A	2	48	26.4	>99	L133A	20	48	86.3	>99
2c	*p*-CH_3	I460V	30	48	59.9	>99	I461V	30	24	72.6	>99
2d	*o*-OCH_3	L134A	10	24	42.5	>99	L133A	50	24	92.5	>99
2e	*m*-OCH_3	L134A	50	48	71.0	>99	L133A	100	3	83.3	>99
2f	*p*-OCH_3	I460V	30	48	19.1	>99	I461V	30	48	63.4	>99
2g	*o*-Br	L256V	70	24	81.6	>99	L257V	100	3	91.7	>99
2h	*m*-Br	I460V	5	24	70.1	98.3	I461V	20	8	91.5	93.4
2i	*p*-Br	I460V	10	24	61.6	>99	I461V	15	6	88.1	>99
2j	*o*-CF_3	L256V	20	24	73.0	>99	L257V	100	3	75.9	>99
2k	*m*-CF_3	I460V	2	24	77.5	>99	I461V	10	8	89.9	>99
2l	*p*-CF_3	I460V	2	48	42.2	>99	I461V	20	48	91.3	>99

*Reaction conditions for amination of **2a-l***: assays were performed in 1.5 mL polypropylene tubes at 30 °C, 250 rpm, in 500 µL reaction volume, using 2-100 mM substrate concentration, (OD_{600}: mM) ratio of 1.0 and 6 M NH_4OH pH 10 (adjusted with CO_2) as reaction medium.

IV.2.1.1.2 Product inhibition

As previously reported[44], I460V *Pc*PAL variant demonstrated low stationary conversion values of 26.4% and 19.1% during the ammonia addition reactions of *m*-methyl-cinnamic acid **2b** and *p*-methoxy-cinnamic acid **2f**, respectively, due to product inhibition. In comparison, I461V *At*PAL variant showed significantly higher stationary conversion values of 86.3% in case of **2b** and 63.4% in case of **2f**, after the same reaction time of 48 h (**Figure IV.5**).

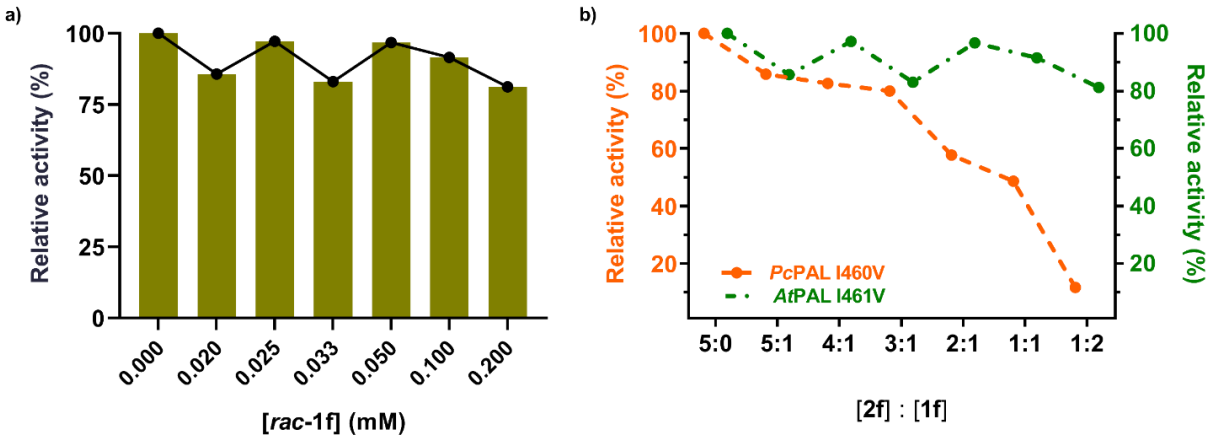

Figure IV.5. a) The influence of increasing product concentration on the relative activity of ammonia addition onto *p*-CH_3O-cinnamic acid **2f** using purified I461V *At*PAL enzyme; b) Comparative UV-assay depletion of *p*-OCH_3-cinnamic acid, at different substrate: product ratios using purified forms of the I461V *At*PAL and I460V *Pc*PAL variant as biocatalysts.

IV.2.1.2 The effect of biocatalyst form

To compare the catalytic performance of wet whole-cells and isolated enzyme PAL biocatalysts, biotransformations of *para*-substituted cinnamic acid derivatives **2c**, **2f**, **2i** and **2l** (chosen as model substrates) were conducted using the I461V and F136V *At*PAL variants, their homologue I460V and F137V *Pc*PAL, in both forms (**Figure IV.6**). This approach aimed to evaluate the extent of differences in biotransformation efficiency between whole-cell and purified enzyme PAL biocatalysts.

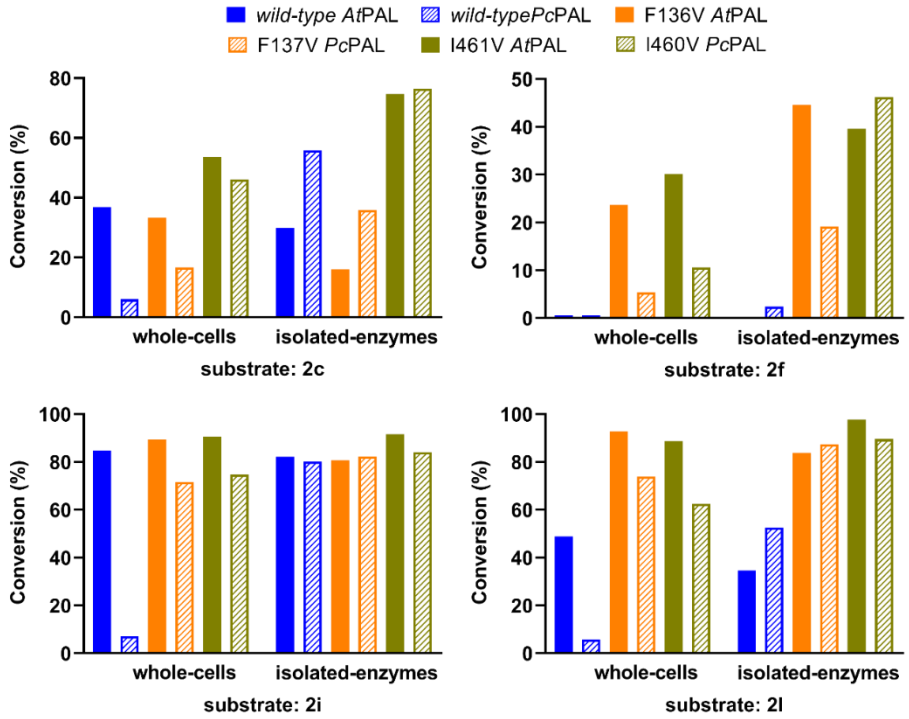

Figure IV.6. Conversion values of the hydroamination of *para*-substituted cinnamic acid derivatives **2c**, **2f**, **2i** and **2l** using wet *whole-cell* and isolated enzyme PAL biocatalysts.

In contrast to *Pc*PAL, which yielded significantly higher conversions using purified enzymes than whole-cell biocatalysts (**Figure IV.7**), *At*PAL did not exhibit a similar trend. Specifically, only the purified form of the best-performing I461V variant resulted in superior conversions, especially in case of substrates bearing electron-donating groups, **2f** and **2c**, where a 1.3- and 1.4-fold increase, respectively was registered when compared to the conversion values provided using *whole-cell* biocatalysts (**Table IV.5**). In general, *whole-cell At*PAL biocatalysts yielded conversions within the same range, or even higher, than those obtained using purified *At*PAL enzymes, indicating higher operational stability. The differences in operational stability and efficiency between *Pc*PAL and *At*PAL proteins may be attributed to their respective tendencies for aggregation and protease stability in their intracellular environment, but also reaction buffer. Lyophilized *whole-cell* PAL biocatalysts were also evaluated and wet whole-cells of *At*PAL I461V variant demonstrated higher conversion efficiency (91%) compared to their lyophilized counterparts (80.5%), while after 48 h (**Table IV.6**). Based on the lower production costs for the *whole-cell* PAL biocatalysts and the competitive conversion values obtained, the wet *whole-cell At*PALs were selected as biocatalysts for further reaction engineering.

Table IV.6. Comparative conversion values of L-**1h** obtained in the ammonia addition reaction using lyophilized *whole-cells* and wet *whole-cells* of *At*PAL I461V variant.

I461V *At*PAL		Time (h)	c (%)
wet *whole-cells*	OD_{600} ~100	24	91.3
		48	88.5
lyophilized cells	20 mg/mL	24	80.5
		48	80.0

Reaction conditions: assays were performed in 1.5 mL polypropylene tubes at 30 °C, 250 rpm for 24-48 h, in 1000 µL reaction volume, using 100 mM substrate concentration (**2h**) and 6 M NH_4OH at pH 10 (adjusted with CO_2) as reaction medium.

IV.2.1.3 The effect of cell density/biocatalyst: substrate ratio

In order to confirm that the previously established biocatalyst: substrate ratio of ~1 (OD_{600}: mM), found to be optimal in our previous work on *Pc*PAL[44], is also optimal for *At*PAL-mediated biotransformations, we conducted further experiments that involved varying the densities of whole-cell biocatalysts (OD_{600} of ~ 1, 2, 4, 8 which correspond to a wet whole-cell concentration of ~ 6, 12, 24 and 48 mg/mL, respectively) while maintaining a fixed substrate concentration of 2 mM for model substrates **2j**, **2e**, and **2i** (**Figure IV.7**).

In all cases, the increase of cell density (OD_{600}>2) did not significantly improve the conversion values, while employing an OD_{600} ≥4 resulted in decreased enantiomeric excess values for L-**1j** (from >99% to 88.2%) and L-**1e** (from >99% to 96.0%) (**Figure IV.7**). Therefore, the results support the optimal biocatalyst: substrate ratio employed for *Pc*PAL-mediated biotransformations to be optimal for *At*PAL-catalyzed ammonia additions ((OD_{600}: mM) ratio ~1).

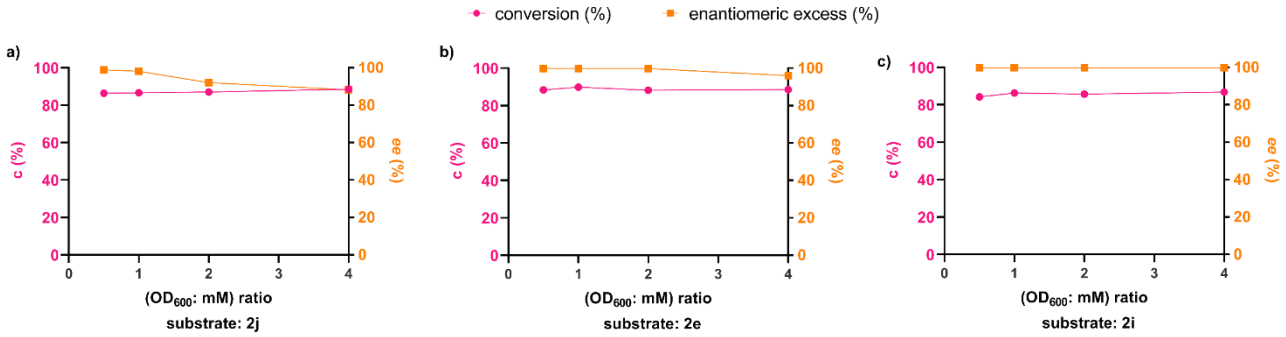

Figure IV.7. Conversion and enantiomeric excess (ee_L) values of the hydroamination of a) *o*-CF_3-cinnamic acid **2j**, b) *m*-OCH_3-cinnamic acid **2e** and c) *p*-Br-cinnamic acid **2i** obtained by varying the biocatalyst: substrate ratio (OD_{600}: mM).

IV.2.1.4 The effect of ammonia source/reaction medium

In our previous reports[44], we demonstrated that the conversions of *Pc*PAL-based amination reactions are significantly influenced by the reaction medium. In this study, the influence of the reaction medium utilized as ammonia source as well as reaction buffer on the conversion and enantiomeric excess values of hydroamination reactions catalyzed by *At*PALs was investigated using two *para*-substituted cinnamic acid derivatives, *p*-methyl-cinnamic acid **2c** and *p*-trifluoromethyl-cinnamic acid **2l** as model substrates (**Figure IV.9**).

The ammonia additions were performed at a fixed substrate concentration of 2 mM and *whole-cell At*PAL I461V-biocatalysts in cell densities of OD_{600} ~ 1 (~6 mg wet cells/mL), varying different

concentration of ammonia buffer solutions (2, 4, 6 M NH_4OH pH 9.5 adjusted with CO_2) and ammonium carbamate buffer solutions (2, 4, 6 M $NH_4[H_2NCO_2]$ pH ~9.5 without adjustment). Higher conversions were achieved with 6 M NH_4OH (66.3% for **2c** and 84.1% for **2l**) or 3-6 M ammonium carbamate for both substrates (**Figure IV.8**). Moreover, in contrast to *Pc*PAL I460V variant[44], the *E. coli* whole-cells harbouring the *At*PAL I461V gene exhibited higher operational stability in the presence of high concentrations of ammonia (c>74% for **2c** and c>92% for **2l**).

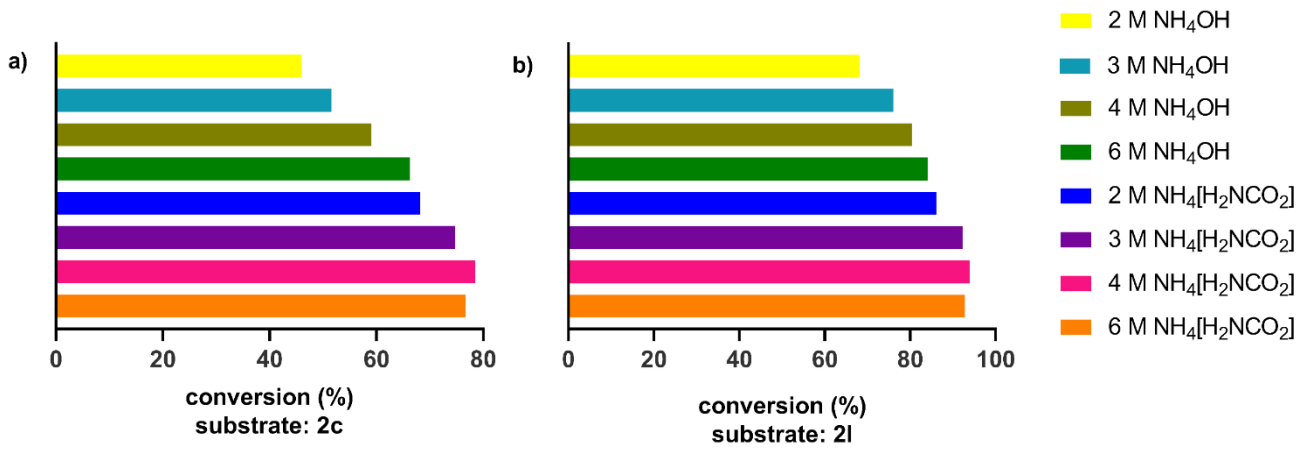

Figure IV.9. Conversion values obtained in the ammonia addition reactions of a) *p*-CH_3-cinnamic acid **2c** and b) *p*-CF_3-cinnamic acid **2l**, using NH_4OH and $NH_4[H_2NCO_2]$ buffers as ammonia sources. In all points of the reactions the enantiomeric excess (ee_L) values were >99%.

IV.2.1.5 The effect of pH

To determine the optimal ammonia source for *At*PAL-catalyzed ammonia additions, we compared the use of NH_4OH and $NH_4[H_2NCO_2]$ buffers in the amination reactions of two model substrates, namely *m*-OCH_3-cinnamic acid **2e** and *p*-Br-cinnamic acid **2i**, more exactly. Specifically, we examined the impact of pH on the conversion values (**Figure IV.9**), at a fixed substrate concentration of 2 mM, using *At*PAL I461V and L133A whole-cells in a biocatalyst: substrate ratio of ~1.

Among the tested ammonia concentrations, 3 M $NH_4[H_2NCO_2]$ was found to be the optimal concentration owing to its unadjusted pH of ~9.5, while 6 M NH_4OH required adjustment with CO_2 to reach a pH range from 8.85 to 11.5. At pH values above 10.0, we observed a significant decrease in conversion values for both substrates, whereas at a pH of ~9.5, we obtained maximum conversion values for all model substrates, regardless of the ammonia source used (**Figure IV.9**).

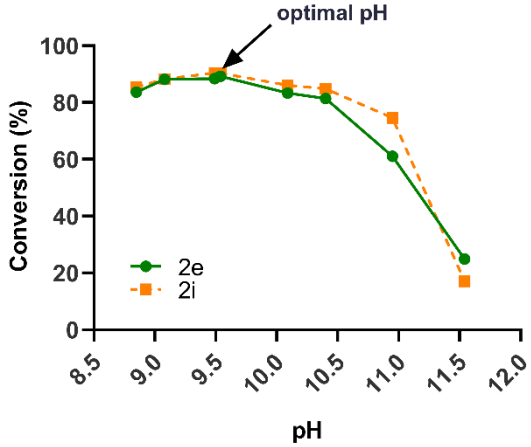

Figure IV.9. Conversion values obtained in the *At*PAL I461V and L133A whole-cells mediated amination reaction of *m*-OCH_3-cinnamic acid **2e** and *p*-Br-cinnamic acid **2i** (pH value ranges from 8.85 to 11.5).

IV.2.1.6 The effect of temperature

We explored the effect of temperature on the conversion values of *whole-cell* biotransformations using **2a**, **2b** and **2c** as model substrates. The ammonia addition reactions were performed at different temperatures (15-45 ºC) and with two substrate concentrations (2 mM and 20 mM), as shown in **Figure IV.10.**

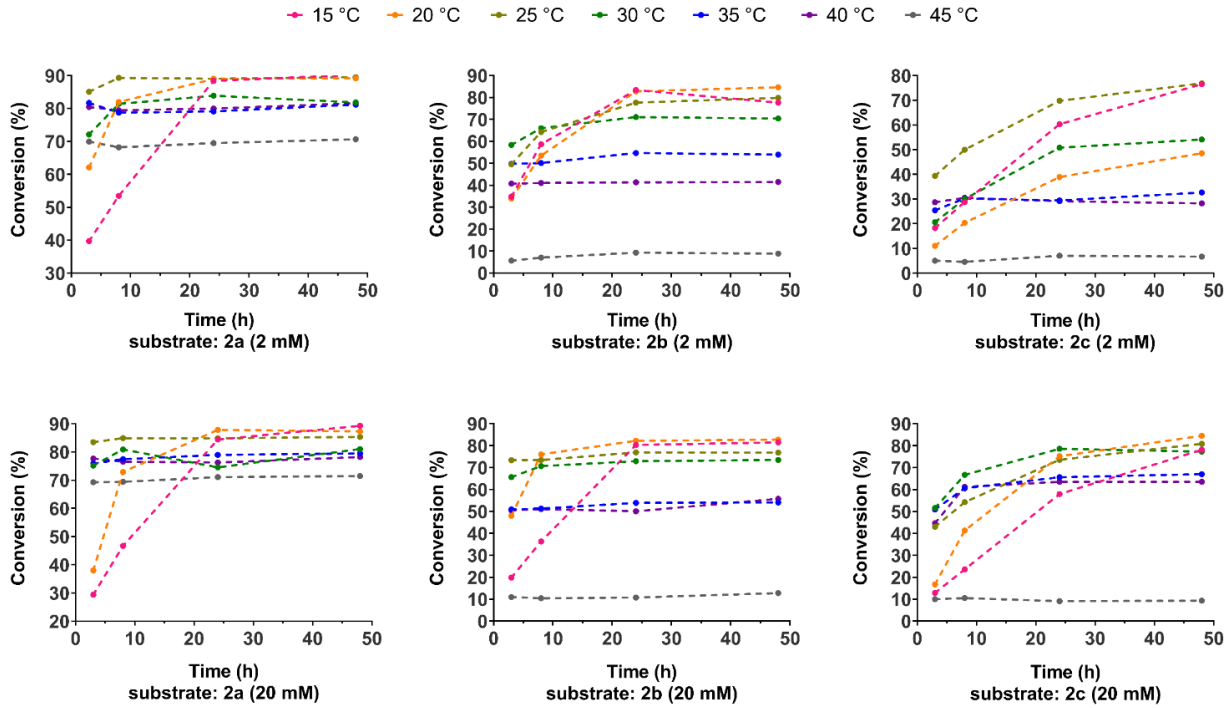

Figure IV.10. The influence of temperature on the conversion values of the *At*PAL-based amination reactions of (*o*-, *m*-, *p*-) substituted methyl-cinnamic acids **2a**, **2b** and **2c** (substrate concentration is indicated in parentheses).

As depicted in **Figure IV.10**, a marked decline in stationary conversion values was observed at temperatures of 40 ºC or 45 ºC for all three substrates, which caused the inactivation of the whole-cell biocatalysts. Although *At*PAL *whole-cells* demonstrated efficiency and stability even at lower temperatures, depending on the substrate, the temperature range of 25-30 ºC was chosen due to its effectiveness with all the tested substrates and ease of maintenance.

IV.2.2 Use of *At*PAL for preparative-scale biotransformations

Preparative-scale biotransformations were performed at 1 gram scale using engineered *At*PAL *whole-cell* biocatalysts under optimal reaction conditions.

Model substrates **2a**, **2b**, **2e**, **2f**, **2g** and **2i** were selected to produce industrially important enantiopure L-phenylalanine analogues (**Figure IV.11**).

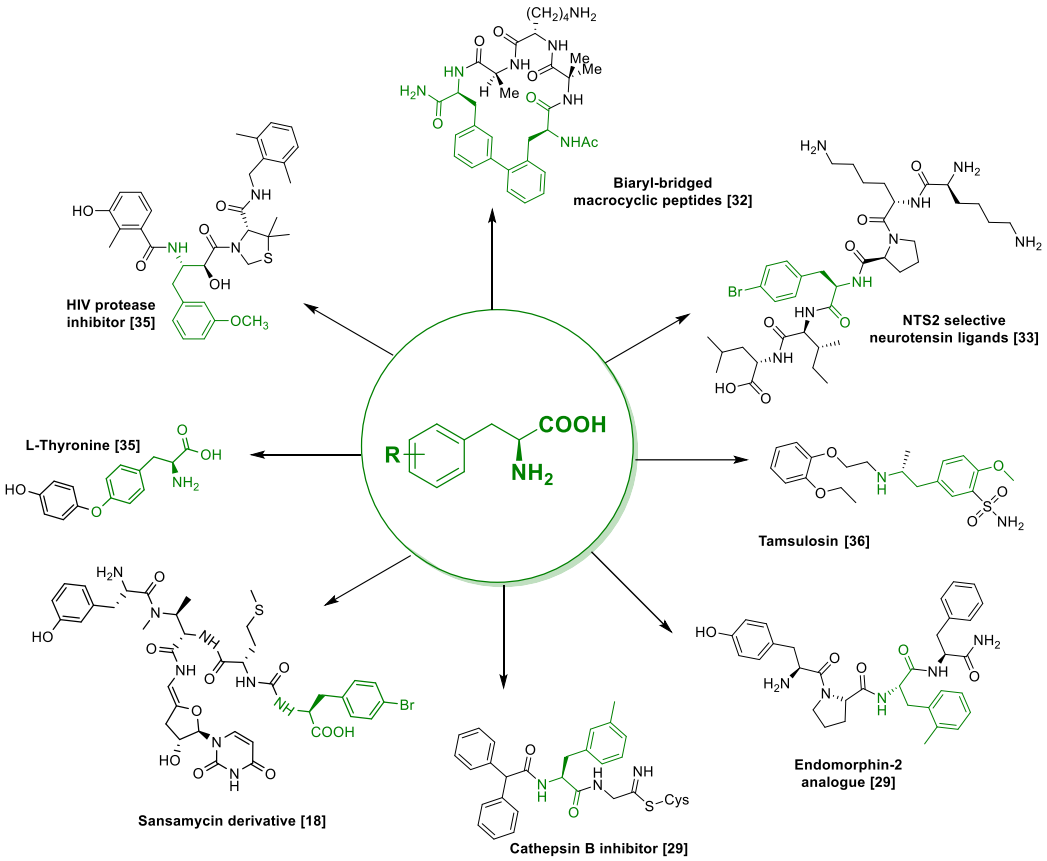

Figure IV.11. Scaled-up production of synthetically valuable phenylalanine analogues as building blocks for active pharmaceutical ingredients (APIs), using *whole-cells* *At*PAL mutant variants.

IV.2.2.1 Preparative-scale results and previously reported PAL-based procedures

After optimizing the reaction conditions, we performed the ammonia addition reactions on cinnamic acid derivatives **2a**, **2g**, **2b**, **2e**, **2f** and **2i** at a 1-gram preparative scale (**Tables IV.3** and **IV.4**). The resulting L-phenylalanine products displayed high optical purities and competitive reaction yields ranging between 56-66% (**Tables IV.12**).

Of particular note was the yield of 66% obtained for L-*m*-OCH_3-Phe L-**1e**, which surpassed the values reported for *Pc*PAL L134A[44] and *Pb*PAL[31] reactions performed at a lower substrate concentration of 30 mM (500 mg-scale) and 50 mM (89 mg-scale), respectively. When compared to the semi-preparative scale reaction (36% yield, 89 mg substrate) mediated by the *Pb*PAL F113Y mutant[45], a 23% increase in reaction yield (59%) was observed at a 1 g preparative-scale for L-*p*-OCH_3-Phe L-**1f** when using *At*PAL I461V wet whole-cells (**Tables IV.3**).

Despite achieving high stationary conversion values in case of L-**1a** and L-**1g** (88% and 95% respectively), the overall yields (66% and 64%) were limited by the product isolation yields, which were calculated considering the conversion value-derived product as maximal quantity.

Table IV.2. Characterization of L-phenylalanine derivatives obtained in the preparative-scale biotransformations with *At*PAL wet *whole-cells*.

Nr crt	L-phenylalanine derivative	*At*PAL variant	conversion [%]	$\eta_{purification}$* [%]	$\eta_{reaction}$# [%]	$[\alpha]_D^{25}$	Product utility
1	L-*o*-CH_3-Phe (L-**1a**)	L257V	88	75	66	-38	μ-opioid receptors[46]; cathepsin B inhibitor[47]

2	L-*o*-Br-Phe (L-**1g**)	L257V	95	67	64	-37	macrocyclic peptides[48]
3	L-*m*-CH_3-Phe (L-**1b**)	L133A	78	83	65	-35	cathepsin B inhibitor[47]; LAT1 inhibitor[49]
4	L-*m*-OCH_3-Phe (L-**1e**)	L133A	87	76	66	-187	HIV protease inhibitor[35]; oxazolidinone antidiabetic[31] caspase inhibitor[50]
5	L-*p*-OCH_3-Phe (L-**1f**)	I461V	72	82	59	-80	tamsulosin[51]; L-thyronine[52]
6	L-*p*-Br-Phe (L-**1i**)	I461V	81	69	56	-27	biarylalanines[34]; sansamycin analogue[36]; hexapeptide agonists[53]

*Purification yield, considering the conversion value-derived product as maximal quantity; #Reaction yield calculated from the preparative-scale reaction including product isolation and purification steps; Optical rotations measurements were performed at room temperature in MeOH with a substrate concentration of 10 mg/mL.

Table IV.3. Preparative-scale production of L-**1a,g,b,e,f,i,l** and comparison to previously reported PAL-procedures results. Results in this work are marked with grey background.

Nr crt	L-Phe derivative product	Scale (g)	Enzyme	[S] (mM)	$\eta_{reaction}$* (%)	ee_L (%)	E factor#	R.t. (h)	Ammonia source
1	L-*o*-CH_3-Phe (L-**1a**)	1	*At*PAL L257V	100	66	>99	32.3	4	3 M $NH_4[H_2NCO_2]$
2	L-*o*-Br-Phe (L-**1g**)	1	*At*PAL L257V	50	64	>99	39.3	4	3 M $NH_4[H_2NCO_2]$
3	L-*m*-CH_3-Phe (L-**1b**)	1	*At*PAL L133A	50	65	>99	50.2	22	3 M $NH_4[H_2NCO_2]$
4	L-*m*-OCH_3-Phe (L-**1e**)	0.5[44]	*Pc*PAL L134A	30	59	>99	79.9	42	6 M NH_4OH
		0.089[31]	*Pb*PAL	50	61	>99	n.r.	24	4 M $NH_4[H_2NCO_2]$
		1	*At*PAL L133A	100	66	>99	28.4	3	3 M $NH_4[H_2NCO_2]$
5	L-*p*-OCH_3-Phe (L-**1f**)	1	*At*PAL I461V	30	59	>99	84.6	48	3 M $NH_4[H_2NCO_2]$
		0.089[45]	*Pb*PAL F113Y	50	36	>99	n.r.	12-16	4 M $NH_4[H_2NCO_2]$
6	L-*p*-Br-Phe (L-**1i**)	0.5[44]	*Pc*PAL I460V	10	82	>99	121.8	48	6 M NH_4OH
		1	*At*PAL I461V	100	56	>99	33.9	24	3 M $NH_4[H_2NCO_2]$
		0.022[34]	*Av*PAL F107A	10	62	-	n.r.	24	5 M NH_4OH

Reaction conditions: assays were performed according to *Chapter V. Experimental Section: Materials and Methods*; #simplified E-factors (sEF). Details in Subchapter IV.2.2.3.; n.r-not reported; R.t.-reaction time; *Reaction yield calculated from the preparative-scale reaction including product isolation and purification steps.

IV.2.2.2 Simplified E-factors (sEF) and space-time yields (STY)

The Simplified E-factors (sEF) were calculated for the *At*PAL-based amination reactions of **2a**, **2b**, **2e**, **2f**, **2g** and **2i** (**Table IV.4**). The values obtained for *m*-MeO-cinnamic acid **2e** and *p*-Br-cinnamic acid **2i** show a 2.8- and 3.6-fold decrease, respectively of SEFs compared to those observed in similar preparative-scale processes based on *Pc*PAL wet whole-cells for the same substrates. In general, lower substrate concentrations led to higher sEF values, which is attributed to the increase in

reaction volume that requires the use of greater quantities of ammonium carbamate buffer. For instance, with *p*-MeO-cinnamic acid **2f** at a substrate concentration of 30 mM, a sEF value of 84.7 was obtained, whereas with *m*-MeO-cinnamic acid **2e** using a substrate concentration of 100 mM gave a sEF value of 28.4 (**Table IV.4**).

Table IV.4. The simplified E-factors (sEFs) and Space-Time Yields (STYs) calculated for the production L-phenylalanine derivatives using *At*PAL wet whole-cells. These results were compared with those obtained through previously reported[44] *Pc*PAL-catalyzed ammonia addition reactions (coloured in orange).

	Products from preparative-scale ammonia addition reactions							
Materials (kg)	**L-*o*-CH_3-Phe (L-1a)**	**L-*o*-Br-Phe (L-1g)**	**L-*m*-CH_3-Phe (L-1b)**	**L-*m*-OCH_3-Phe (L-1e)**	**L-*p*-OCH_3-Phe (L-1f)**	**L-*p*-Br-Phe (L-1i)**	**L-*m*-OCH_3-Phe (L-1e)***	**L-*p*-Br-Phe (L-1i)**
Acrylic acid	1.44	1.50	1.37	1.39	1.66	2.03	1.71	1.24
L-amino acid	1.00	1.00	1.00	1.00	1.00	1.00	1.00	1.00
$[NH_4][CO_2NH_2]$	20.77	30.90	10.14	18.26	72.72	20.9	67.23[#]	114.80[#]
PAL cells	11.10	7.90	39.69	9.80	11.30	11.06	12	6.75
sEF	**32.3**	**39.3**	**50.2**	**28.4**	**84.7**	**33.9**	**79.9**	**121.8**
STY ($g*L^{-1}*d^{-1}$)	**66.2**	**44.3**	**6.4**	**101.3**	**1.6**	**10.9**	**1.7**	**0.9**

Reaction conditions: assays were performed according to *Chapter V. Experimental Section: Materials and Methods.* *Calculated from previously reported[44] *Pc*PAL-catalyzed ammonia addition reactions. [#]6 M NH_4OH buffer (pH 9.5 adjusted with CO_2) as reaction medium

Space-Time Yield values (STYs), were calculated for the *At*PAL-based ammonia addition reactions of **2a**, **2b**, **2e**, **2f**, **2g** and **2i** (**Table IV.5**) and were compared to other previously reported PAL-based technologies used for the synthesis of various L-phenylalanine derivatives, including (*R*)-2-amino-3-(2-(benzyloxy)-3-methoxyphenyl)propanoic acid[25], L-3-fluoro-phenylalanine[27] and L-2-chloro-phenylalanine[24, 27].

Table IV.5. Space-time yield values of several reported PAL-based technologies.

Materials	**DSM[24]**	**Novartis[25]**	**N.J. Turner's group[27]**
Starting material (g)	28.0	20.0	1.0
Conversion (%)	91.0	76.0	92.0
Product (g)	18.0	16.1	1.0
Time (h)	8.5	96.0	6.0
Volume (mL)	1000.0	170.0	17.0
STY ($g*L^{-1}*d^{-1}$)	**51.2[27]**	**23.7**	**237.6**

V.3 Conclusions

This study presents highly efficient biocatalytic procedures for the synthesis of industrially significant L-phenylalanine analogues through the utilization of mutant variants of phenylalanine ammonia-lyases derived from *Arabidopsis thaliana*. Our results indicate that *At*PAL *whole-cell*

biocatalysts outperform the previously studied *Pc*PAL homologues in terms of overcoming substrate and product inhibition, achieving higher conversions, enantiomeric excess values, and shorter reaction times even at higher substrate concentrations (up to 100 mM).

By employing various reaction engineering strategies, such as optimizing the reaction medium, increasing substrate concentrations, shortening reaction times and achieving higher stationary conversions, we have developed a scalable synthetic protocol for synthesizing several industrially relevant L-phenylalanine analogues such as (*S*)-*o*-CH_3-phenylalanine, (*S*)-*o*-Br-phenylalanine, (*S*)-*m*-OCH_3-phenylalanine, (*S*)-*m*-CH_3-phenylalanine, (*S*)-*p*-OCH_3-phenylalanine and (*S*)-*p*-Br-phenylalanine.

Our approach surpasses the performance of previously reported scaled-up biotransformations using phenylalanine ammonia-lyase and results in improved space-time yield and reduced environmental impact. Successful implementation of the PAL-based procedures described in this study could substantially contribute to the development of processes for synthesizing active pharmaceutical ingredients (APIs) and promote a more environmentally sustainable approach to chemical development using *whole-cell* PALs.

General conclusions

Mutant variants of phenylalanine ammonia-lyase from *Petroselinum crispum* (*Pc*PAL) have been utilized as biocatalysts for the biocatalytic synthesis of L- and D-phenylalanine analogues with high synthetic value. These *Pc*PAL mutants were designed specifically for mono-substituted phenylalanine and cinnamic acid substrates. The study aimed to optimize the catalytic performance of the engineered *Pc*PAL variants by investigating the ammonia elimination and ammonia addition reactions, and examining the impact of key variables such as substrate concentration, biocatalyst: substrate ratio, reaction buffer and reaction time on conversion and enantiomeric excess values. The results demonstrated that an efficient preparative-scale biocatalytic procedure could be developed under optimal conditions. Valuable phenylalanine derivatives were successfully synthesized using this approach, including (*S*)-*m*-OCH_3-phenylalanine (40% yield, ee_S> 99%), (*S*)-*m*-CF3-phenylalanine (26% yield, ee_S> 99%), (*S*)-*p*-Br-phenylalanine (82% yield, ee_S> 99%), (*R*)-*m*-CF_3-phenylalanine (34% yield, ee_R = 93%). (*R*)-*p*-CH_3-phenylalanine (49% yield, ee_R = 95%).

We investigated the transferability of the rational design model for phenylalanine ammonia-lyases of different origins, including *Arabidopsis thaliana* (*At*PAL) and *Rhodosporidium toruloides* (*Rt*PAL), which possess a sequence identity of 81% and 38%, respectively, with *Pc*PAL. Our results suggest that, with some exceptions, the positions of substrate specificity modulating amino acid residues are conserved among the tested phenylalanine ammonia-lyases, allowing the prediction of mutations that enhance PAL activity towards a targeted non-natural substrate. Therefore, our study supports the use of a general approach to modify PALs from different sources with varying substrate scopes. Our findings also reveal that factors other than catalytic site differences can influence PAL activity. For instance, the *At*PAL variants L257V, L133A and I461V exhibited greater catalytic efficiency than their *Pc*PAL counterparts, despite having identical catalytic sites.

Through the use of mutant variants of phenylalanine ammonia-lyase from *Arabidopsis thaliana* (*At*PAL), we have developed a highly efficient preparative scale synthetic procedure for L-phenylalanine derivatives, with improved E-factor and space-time yields, which align with the principles of sustainable and green chemistry. The *At*PAL-based biotransformations of cinnamic acids derivatives has yielded various unnatural amino acids which possess significant potential building blocks for active pharmaceutical ingredients (APIs), including (*S*)-*o*-CH_3-phenylalanine, (*S*)-*o*-Br-phenylalanine, (*S*)-*m*-OCH_3-phenylalanine, (*S*)-*m*-CH_3-phenylalanine, (*S*)-*p*-OCH_3-phenylalanine and (*S*)-*p*-Br-phenylalanine, with superior conversions and yields compared to previously reported *Pc*PAL-based aminations. For this purpose, we have conducted a comprehensive optimization of reaction engineering, including factors such as reaction medium/ammonia source, pH, biocatalyst: substrate ratio, temperature, biocatalyst form, and substrate concentration, to determine the optimal conditions for gram-scale biotransformations.

Chapter V. Experimental section: Materials and Methods

Bibliography

1. Clemente-Jiménez, J. M.; Martínez-Rodríguez, S.; Rodríguez-Vico, F.; Heras-Vázquez, F. J., Optically pure alpha-amino acids production by the "Hydantoinase Process". *Recent Patents on Biotechnology* **2008,** *2* (1), 35-46.
2. Narancic, T.; Almahboub, S. A.; O'Connor, K. E., Unnatural amino acids: production and biotechnological potential. *World journal of Microbiology & Biotechnology* **2019,** *35* (4), 67.
3. Dougherty, D. A., Unnatural amino acids as probes of protein structure and function. *Current Opinion in Chemical Biology* **2000,** *4* (6), 645-652.
4. Axup, J. Y.; Bajjuri, K. M.; Ritland, M.; Hutchins, B. M.; Kim, C. H.; Kazane, S. A.; Halder, R.; Forsyth, J. S.; Santidrian, A. F.; Stafin, K.; Lu, Y.; Tran, H.; Seller, A. J.; Biroc, S. L.; Szydlik, A.; Pinkstaff, J. K.; Tian, F.; Sinha, S. C.; Felding-Habermann, B.; Smider, V. V.; Schultz, P. G., Synthesis of site-specific antibody-drug conjugates using unnatural amino acids. *Proceedings of the National Academy of Sciences of the United States of America* **2012,** *109* (40), 16101-16106.
5. Blaskovich, M. A. T., Unusual amino acids in medicinal chemistry. *Journal of Medicinal Chemistry* **2016,** *59* (24), 10807-10836.
6. Leuchtenberger, W.; Huthmacher, K.; Drauz, K., Biotechnological production of amino acids and derivatives: current status and prospects. *Applied Microbiology and Biotechnology* **2005,** *69* (1), 1-8.
7. May, O.; Verseck, S.; Bommarius, A.; Drauz, K., Development of dynamic kinetic resolution processes for biocatalytic production of natural and nonnatural L-amino acids. *Organic Process Research & Development* **2002,** *6* (4), 452-457.
8. Mollica, A.; Mirzaie, S.; Costante, R.; Carradori, S.; Macedonio, G.; Stefanucci, A.; Dvoracsko, S.; Novellino, E., Exploring the biological consequences of conformational changes in aspartame models containing constrained analogues of phenylalanine. *Journal of Enzyme Inhibition and Medicinal Chemistry* **2016,** *31* (6), 953-963.
9. Chattopadhyay, S.; Raychaudhuri, U.; Chakraborty, R., Artificial sweeteners - a review. *Journal of Food Science and Technology* **2014,** *51* (4), 611-621.
10. Gillbro, J. M.; Olsson, M. J., The melanogenesis and mechanisms of skin-lightening agents-existing and new approaches. *International Journal of Cosmetic Science* **2011,** *33* (3), 210-221.
11. Kochhar, J. S.; Chan, S. Y.; Ong, P. S.; Kang, L., Clinical therapeutics for phenylketonuria. *Drug Delivery and Translational Research* **2012,** *2* (4), 223-237.
12. Thomas, J.; Levy, H.; Amato, S.; Vockley, J.; Zori, R.; Dimmock, D.; Harding, C. O.; Bilder, D. A.; Weng, H. H.; Olbertz, J.; Merilainen, M.; Jiang, J.; Larimore, K.; Gupta, S.; Gu, Z.; Northrup, H., Pegvaliase for the treatment of phenylketonuria: Results of a long-term phase 3 clinical trial program (PRISM). *Molecular Genetics and Metabolism* **2018,** *124* (1), 27-38.
13. Levy, H. L.; Sarkissian, C. N.; Scriver, C. R., Phenylalanine ammonia lyase (PAL): From discovery to enzyme substitution therapy for phenylketonuria. *Molecular Genetics and Metabolism* **2018,** *124* (4), 223-229.
14. Hodgins, D. S., Yeast phenylalanine ammonia-lyase. Purification, properties, and the identification of catalytically essential dehydroalanine. *The Journal of Biological Chemistry* **1971,** *246* (9), 2977-2985.

15. Calabrese, J. C.; Jordan, D. B.; Boodhoo, A.; Sariaslani, S.; Vannelli, T., Crystal structure of phenylalanine ammonia lyase: Multiple helix dipoles implicated in catalysis. *Biochemistry* **2004,** *43* (36), 11403-11416.
16. Ritter, H.; Schulz, G. E., Structural basis for the entrance into the phenylpropanoid metabolism catalyzed by phenylalanine ammonia-lyase. *Plant Cell* **2004,** *16* (12), 3426-3436.
17. Baedeker, M.; Schulz, G. E., Overexpression of a designed 2.2 kb gene of eukaryotic phenylalanine ammonia-lyase in *Escherichia coli*. *FEBS Letters* **1999,** *457* (1), 57-60.
18. Moffitt, M. C.; Louie, G. V.; Bowman, M. E.; Pence, J.; Noel, J. P.; Moore, B. S., Discovery of two cyanobacterial phenylalanine ammonia lyases: kinetic and structural characterization. *Biochemistry* **2007,** *46* (4), 1004-1012.
19. Rétey, J.; Paizs, C.; Tosa, M.; Laszlo Csaba, B.; Brem, J.; Irimie, F. D., 2-Amino-3-(5-phenylfuran-2-yl)propionic Acids and 5-Phenylfuran-2-ylacrylic acids are novel substrates of phenylalanine ammonia-lyase. *Heterocycles* **2010,** *82*, 1217.
20. Paizs, C.; Katona, A.; Rétey, J., The interaction of heteroaryl-acrylates and alanines with phenylalanine ammonia-lyase from parsley. *Chemistry - A European Journal* **2006,** *12* (10), 2739-2744.
21. Bencze, L. C.; Filip, A.; Banoczi, G.; Tosa, M. I.; Irimie, F. D.; Gellert, A.; Poppe, L.; Paizs, C., Expanding the substrate scope of phenylalanine ammonia-lyase from *Petroselinum crispum* towards styrylalanines. *Organic & Biomolecular Chemistry* **2017,** *15* (17), 3717-3727.
22. Filip, A.; Nagy, E. Z. A.; Tork, S. D.; Banoczi, G.; Tosa, M. I.; Irimie, F. D.; Poppe, L.; Paizs, C.; Bencze, L. C., Tailored mutants of phenylalanine ammonia-lyase from *Petroselinum crispum* for the synthesis of bulky L- and D-arylalanines. *ChemCatChem* **2018,** *10* (12), 2627-2633.
23. Nagy, E. Z. A.; Tork, S. D.; Lang, P. A.; Filip, A.; Irimie, F. D.; Poppe, L.; Tosa, M. I.; Schofield, C. J.; Brem, J.; Paizs, C.; Bencze, L. C., Mapping the hydrophobic substrate binding site of phenylalanine ammonia-lyase from *Petroselinum crispum*. *Acs Catalysis* **2019,** *9* (9), 8825-8834.
24. de Lange, B.; Hyett, D. J.; Maas, P. J. D.; Mink, D.; van Assema, F. B. J.; Sereinig, N.; de Vries, A. H. M.; de Vries, J. G., Asymmetric synthesis of (*S*)-2-indolinecarboxylic acid by combining biocatalysis and homogeneous catalysis. *ChemCatChem* **2011,** *3* (2), 289-292.
25. Hardegger, L. A.; Beney, P.; Bixel, D.; Fleury, C.; Gao, F.; Perrenoud, A. G.-G.; Gu, X.; Haber, J.; Hong, T.; Humair, R.; Kaegi, A.; Kibiger, M.; Kleinbeck, F.; Luu, V. T.; Padeste, L.; Rampf, F. A.; Ruch, T.; Schlama, T.; Sidler, E.; Udvarhelyi, A.; Wietfeld, B.; Yang, Y., Toward a scalable synthesis and process for EMA401, Part III: Using an engineered phenylalanine ammonia lyase enzyme to synthesize a non-natural phenylalanine derivative. *Organic Process Research & Development* **2020,** *24* (9), 1763-1771.
26. Rowles, I.; Groenendaal, B.; Binay, B.; Malone, K. J.; Willies, S. C.; Turner, N. J., Engineering of phenylalanine ammonia lyase from *Rhodotorula graminis* for the enhanced synthesis of unnatural L-amino acids. *Tetrahedron* **2016,** *72* (46), 7343-7347.
27. Weise, N. J.; Ahmed, S. T.; Parmeggiani, F.; Siirola, E.; Pushpanath, A.; Schell, U.; Turner, N. J., Intensified biocatalytic production of enantiomerically pure halophenylalanines from acrylic acids using ammonium carbamate as the ammonia source. *Catalysis Science and Technology* **2016,** *6* (12), 4086-4089.
28. Hyun, M. W.; Yun, Y. H.; Kim, J. Y.; Kim, S. H., Fungal and plant phenylalanine ammonia-lyase. *Mycobiology* **2011,** *39* (4), 257-265.
29. Zhang, F.; Huang, N.; Zhou, L.; Cui, W.; Liu, Z.; Zhu, L.; Liu, Y.; Zhou, Z., Modulating the pH activity profiles of phenylalanine ammonia lyase from *Anabaena variabilis* by modification of center-near surface residues. *Applied Biochemistry and Biotechnology* **2017,** *183* (3), 699-711.
30. Weise, N. J.; Parmeggiani, F.; Ahmed, S. T.; Turner, N. J., Discovery and investigation of mutase-like activity in a phenylalanine ammonia lyase from *Anabaena variabilis*. *Top Catalysis* **2018,** *61* (3-4), 288-295.
31. Weise, N. J.; Ahmed, S. T.; Parmeggiani, F.; Galman, J. L.; Dunstan, M. S.; Charnock, S. J.; Leys, D.; Turner, N. J., Zymophore identification enables the discovery of novel phenylalanine ammonia lyase enzymes. *Scientific Reports* **2017,** *7*, 13691.

32. Ahmed, S. T.; Parmeggiani, F.; Weise, N. J.; Flitsch, S. L.; Turner, N. J., Engineered ammonia lyases for the production of challenging electron-rich l-phenylalanines. *ACS Catalysis* **2018,** *8* (4), 3129-3132.
33. Parmeggiani, F.; Lovelock, S. L.; Weise, N. J.; Ahmed, S. T.; Turner, N. J., Synthesis of D- and L-phenylalanine derivatives by phenylalanine ammonia lyases: A multienzymatic cascade process. *Angewandte Chemie International Edition* **2015,** *54* (15), 4608-4611.
34. Ahmed, S. T.; Parmeggiani, F.; Weise, N. J.; Flitsch, S. L.; Turner, N. J., Chemoenzymatic synthesis of optically pure L- and D-biarylalanines through biocatalytic asymmetric amination and palladium-catalyzed arylation. *ACS Catalysis* **2015,** *5* (9), 5410-5413.
35. Mimoto, T.; Terashima, K.; Nojima, S.; Takaku, H.; Nakayama, M.; Shintani, M.; Yamaoka, T.; Hayashi, H., Structure-activity and structure-metabolism relationships of HIV protease inhibitors containing the 3-hydroxy-2-methylbenzoyl-allophenylnorstatine structure. *Bioorganic & Medicinal Chemistry* **2004,** *12* (1), 281-93.
36. Zhang, N.; Liu, L.; Shan, G.; Cai, Q.; Lei, X.; Hong, B.; Wu, L.; Xie, Y.; Chen, R., Precursor-directed biosynthesis of new sansanmycin analogs bearing para-substituted-phenylalanines with high yields. *The Journal of Antibiotics* **2016,** *69* (10), 765-768.
37. Yang, B.; Lamb, M. L.; Zhang, T.; Hennessy, E. J.; Grewal, G.; Sha, L.; Zambrowski, M.; Block, M. H.; Dowling, J. E.; Su, N.; Wu, J.; Deegan, T.; Mikule, K.; Wang, W.; Kaspera, R.; Chuaqui, C.; Chen, H., Discovery of potent KIFC1 inhibitors using a method of integrated high-throughput synthesis and screening. *Journal of Medicinal Chemistry* **2014,** *57* (23), 9958-9970.
38. Dong, L.; Marakovits, J.; Hou, X.; Guo, C.; Greasley, S.; Dagostino, E.; Ferre, R.; Johnson, M. C.; Kraynov, E.; Thomson, J.; Pathak, V.; Murray, B. W., Structure-based design of novel human Pin1 inhibitors (II). *Bioorganic & Medicinal Chemistry Letters* **2010,** *20* (7), 2210-2214.
39. Hwang, T. L.; Hung, C. H.; Hsu, C. Y.; Huang, Y. T.; Tsai, Y. C.; Hsieh, P. W., Design and synthesis of tryptophan containing dipeptide derivatives as formyl peptide receptor 1 antagonist. *Organic & Biomolecular Chemistry* **2013,** *11* (22), 3742-3755.
40. Lenstra, D. C.; Damen, E.; Leenders, R. G. G.; Blaauw, R. H.; Rutjes, F.; Wegert, A.; Mecinović, J., Structure-activity relationship studies on (*R*)-PFI-2 analogues as inhibitors of histone lysine methyltransferase SETD7. *ChemMedChem* **2018,** *13* (14), 1405-1413.
41. Lovelock, S. L.; Turner, N. J., Bacterial *Anabaena variabilis* phenylalanine ammonia lyase: A biocatalyst with broad substrate specificity. *Bioorganic and Medicinal Chemistry* **2014,** *22* (20), 5555-5557.
42. Tork, S. D.; Moisă, M. E.; Cserepes, L.; Filip, A.; Nagy, L. C.; Irimie, F. D.; Bencze, L. C., Towards a general approach for tailoring the hydrophobic binding site of phenylalanine ammonia-lyases. *Scientific Reports* **2022,** *12* (1), 10606.
43. Tork, S. D.; Nagy, E. Z. A.; Cserepes, L.; Bordea, D. M.; Nagy, B.; Tosa, M. I.; Paizs, C.; Bencze, L. C., The production of L- and D-phenylalanines using engineered phenylalanine ammonia lyases from *Petroselinum crispum*. *Scientific Reports* **2019,** *9*, 20123.
44. Li, T.; Shiotani, K.; Miyazaki, A.; Tsuda, Y.; Ambo, A.; Sasaki, Y.; Jinsmaa, Y.; Marczak, E.; Bryant, S. D.; Lazarus, L. H.; Okada, Y., Bifunctional [2',6'-dimethyl-L-tyrosine1]endomorphin-2 analogues substituted at position 3 with alkylated phenylalanine derivatives yield potent mixed mu-agonist/delta-antagonist and dual mu-agonist/delta-agonist opioid ligands. *Journal of Medicinal Chemistry* **2007,** *50* (12), 2753-2766.
45. Schmitz, J.; Gilberg, E.; Löser, R.; Bajorath, J.; Bartz, U.; Gütschow, M., Cathepsin B: Active site mapping with peptidic substrates and inhibitors. *Bioorganic & Medicinal Chemistry* **2019,** *27* (1), 1-15.
46. Cawley, N. X.; Huang, J.; Peng Loh, Y.; Dhanvantari, S., Prohormone convertases. In *Reference Module in Biomedical Sciences*, Elsevier: **2014**.
47. Chien, H. C.; Colas, C.; Finke, K.; Springer, S.; Stoner, L.; Zur, A. A.; Venteicher, B.; Campbell, J.; Hall, C.; Flint, A.; Augustyn, E.; Hernandez, C.; Heeren, N.; Hansen, L.; Anthony, A.; Bauer, J.; Fotiadis,

D.; Schlessinger, A.; Giacomini, K. M.; Thomas, A. A., Reevaluating the Substrate Specificity of the L-Type Amino Acid Transporter (LAT1). *Journal of Medicinal Chemistry* **2018,** *61* (16), 7358-7373.
48. Vickers, C. J.; González-Páez, G. E.; Wolan, D. W., Selective detection of caspase-3 versus caspase-7 using activity-based probes with key unnatural amino acids. *ACS Chemical Biology* **2013,** *8* (7), 1558-1566.
49. Arava, V. R.; Amasa, S. R.; Goud Bhatthula, B. K.; Kompella, L. S.; Matta, V. P.; Subha, M. C. S., Asymmetric Synthesis of Unnatural Amino Acids and Tamsulosin Chiral Intermediate. *Synthetic Communications* **2013,** *43* (21), 2892-2897.
50. Carrel, T.; Eckstein, F.; Englberger, L.; Mury, R.; Mohacsi, P., Thyronin treatment in adult and pediatric heart surgery: clinical experience and review of the literature. *European Journal of Heart Failure* **2002,** *4* (5), 577-582.
51. Simeth, N. A.; Bause, M.; Dobmeier, M.; Kling, R. C.; Lachmann, D.; Hübner, H.; Einsiedel, J.; Gmeiner, P.; König, B., NTS2-selective neurotensin mimetics with tetrahydrofuran amino acids. *Bioorganic & Medicinal Chemistry* **2017,** *25* (1), 350-359.
52. Ahmed, S. T.; Parmeggiani, F.; Weise, N. J.; Flitsch, S. L.; Turner, N. J., Engineered ammonia lyases for the production of challenging electron-rich l-phenylalanines. *ACS Catalysis* **2018,** *8* (4), 3129-3132.